JEM Journal of Experimental Medicine

ARTICLE

The human fetal thymus generates invariant effector γδ T cells

Paola Tieppo[1,2], Maria Papadopoulou[1,2], Deborah Gatti[1,2], Naomi McGovern[3], Jerry K.Y. Chan[4,5,6], Françoise Gosselin[7], Glenn Goetgeluk[8], Karin Weening[8], Ling Ma[1,2], Nicolas Dauby[2,9], Alexandra Cogan[10], Catherine Donner[7], Florent Ginhoux[11], Bart Vandekerckhove[8], and David Vermijlen[1,2]

In the mouse thymus, invariant γδ T cells are generated at well-defined times during development and acquire effector functions before exiting the thymus. However, whether such thymic programming and age-dependent generation of invariant γδ T cells occur in humans is not known. Here we found that, unlike postnatal γδ thymocytes, human fetal γδ thymocytes were functionally programmed (e.g., IFNγ, granzymes) and expressed low levels of terminal deoxynucleotidyl transferase (TdT). This low level of TdT resulted in a low number of N nucleotide insertions in the complementarity-determining region-3 (CDR3) of their TCR repertoire, allowing the usage of short homology repeats within the germline-encoded VDJ segments to generate invariant/public cytomegalovirus-reactive CDR3 sequences (TRGV8-TRJP1-CATWDTTGWFKIF, TRDV2-TRDD3-CACDTGGY, and TRDV1-TRDD3-CALGELGD). Furthermore, both the generation of invariant TCRs and the intrathymic acquisition of effector functions were due to an intrinsic property of fetal hematopoietic stem and precursor cells (HSPCs) caused by high expression of the RNA-binding protein Lin28b. In conclusion, our data indicate that the human fetal thymus generates, in an HSPC/Lin28b-dependent manner, invariant γδ T cells with programmed effector functions.

Introduction

γδ T cells have been conserved since the emergence of jawed vertebrates >450 million years ago alongside B cells and αβ T cells and play an important role in antimicrobial and antitumor immunity (Hayday, 2000; Chien et al., 2014; Silva-Santos et al., 2015). Like αβ T cells and B cells, γδ T cells use V(D)J (V, variable; D, diversity; J, joining) gene rearrangement with the potential to generate a set of highly diverse receptors to recognize antigens. This diversity is generated mainly in the complementarity-determining region 3 (CDR3) of the TCR formed by V(D)J gene rearrangements in the TRG and TRD loci. A high level of junctional diversity is caused by the random insertion of nucleotides (denoted by N) by the enzyme terminal deoxynucleotidyl transferase (TdT) into the junctions of the joining gene segments (Chien and Konigshofer, 2007). Mainly based on findings in the mouse model, γδ T cells are regarded as innate T cells. Indeed, waves of γδ T cell subsets are generated in the mouse thymus, especially before birth, that possess invariant TCRs (i.e., the same CDR3γ and CDR3δ sequences) and programmed effector functions, such as invariant Vγ5Vδ1 T cells that home to the skin epidermis as dendritic epidermal T cells (Havran and Allison, 1990; Ikuta et al., 1990; Vermijlen and Prinz, 2014). After birth, a more diverse γδ TCR repertoire is generated, but thymic programming (IL17 versus IFNγ effector dichotomy) is still present (Ribot et al., 2009; Muñoz-Ruiz et al., 2016). In contrast, human γδ thymocytes, at least postnatally, do not show such a functional commitment (Ribot et al., 2014). Further arguing against the generation of "innate" γδ T cells in the human thymus is the recent finding that the TRG and TRD repertoire of human pediatric thymuses and of term-delivery cord blood (CB) is highly polyclonal (Ravens et al., 2017; Davey et al., 2017; Kallemeijn et al., 2018; Silva-Santos and Strid, 2017; Di Lorenzo et al., 2017, 2019). In adults, the γδ TCR repertoire in the peripheral blood becomes less diverse and highly focused, highlighting the potential adaptive function of human γδ T cells

[1]Department of Pharmacotherapy and Pharmaceutics, Université Libre de Bruxelles (ULB), Bruxelles, Belgium; [2]Institute for Medical Immunology, Université Libre de Bruxelles (ULB), Gosselies, Belgium; [3]Department of Pathology and Centre for Trophoblast Research, University of Cambridge, Cambridge, UK; [4]Department of Reproductive Medicine, KK Women's and Children's Hospital, Singapore; [5]Department of Obstetrics & Gynaecology, Yong Loo Lin School of Medicine, National University of Singapore, Singapore; [6]OBGYN-Academic Clinical Program, Duke-National University of Singapore, Duke-National University of Singapore Medical School, Singapore; [7]Department of Obstetrics and Gynecology, Hôpital Erasme, Université Libre de Bruxelles (ULB), Bruxelles, Belgium; [8]Department of Clinical Chemistry, Microbiology and Immunology, Ghent University, Ghent, Belgium; [9]Department of Infectious Diseases, Centre Hospitalier Universitaire Saint-Pierre, Université Libre de Bruxelles (ULB), Bruxelles, Belgium; [10]Department of Obstetrics and Gynecology, Centre Hospitalier Universitaire Saint-Pierre, Université Libre de Bruxelles (ULB), Bruxelles, Belgium; [11]Singapore Immunology Network, Agency for Science, Technology and Research, Singapore.

Correspondence to David Vermijlen: dvermijl@ulb.ac.be.

(Ravens et al., 2017; Davey et al., 2017; Silva-Santos and Strid, 2017). Thus, it is not clear whether thymic programming of γδ T cells exists in humans, further contributing to the notion that mouse and human γδ T cells are different (Mestas and Hughes, 2004; Pang et al., 2012; Van de Walle et al., 2009), possibly because human TCRs have an inherent bias to N-containing CDR3 regions (Chen et al., 2017).

Immune cells are generated by hematopoietic stem and precursor cells (HSPCs). In the mouse model, evidence has been obtained for the developmentally ordered appearance (or "layered development") of distinct HSPCs that give rise to distinct immune cell lineages at different stages of development, including the generation of innate lymphocytes such as dendritic epidermal T cells and B1 lymphocytes (Ikuta et al., 1990; Havran and Allison, 1990; Yuan et al., 2012; Ginhoux and Jung, 2014; Beaudin et al., 2016; Ramond et al., 2014; Gentek et al., 2018; Kreslavsky et al., 2018; Smith et al., 2018). However, other studies indicate that the available niche at the time of development is more important (van de Laar et al., 2016). Whether a layered production of innate lymphocytes exists in humans is not known. Indeed, human fetal HSPCs are rather biased toward the generation of regulatory T cells, thus contributing to immune tolerance in the fetus (Mold et al., 2010).

Here, we found that the human fetal thymus (FT) generates γδ T cells with invariant human CMV-reactive TCRs and programmed effector functions. Our data support the concept of a layered development as human fetal but not adult HSPCs could reproduce the generation of such innate γδ T cells. Finally, a key role for the RNA-binding protein Lin28b was demonstrated in the generation of human innate γδ T cells, both at the functional and TCR/CDR3 level.

Results

Human fetal γδ thymocytes express an effector program

Analyzing γδ thymocytes from pediatric thymuses (newborn to 9-yr-old children), Ribot et al. (2014) did not find evidence (e.g., no IFNγ expression) for functional programming. Since functional programming of mouse γδ thymocytes is especially present at the time the first mouse T cells are generated (late gestation/perinatally), and since T cell development starts in humans well before birth (Lewis and Wilson, 2006; Vermijlen and Prinz, 2014), we investigated this issue in human FT samples. We sorted γδ (without the Vγ9Vδ2 subset; see Materials and methods) and αβ T cells from FT samples (17–19 wk gestation) and compared their gene expression profiles with their counterparts sorted from pediatric/postnatal thymuses (PNTs; 4 mo–8 yr). Comparing these gene expression profiles in an unbiased manner with a vast database of existing immune cell–associated gene sets (the Molecular Signatures Database [MSigDB] containing 4,872 immunological signatures; Godec et al., 2016) revealed that FT γδ thymocytes share a gene expression program with activated T cells (both in human and mouse gene sets; Fig. 1 A). Furthermore, a high sharing with IL15-stimulated gene expression in natural killer (NK) cells was identified, again both in humans and mice (Fig. 1 A). Fetal γδ thymocytes clearly expressed IFNγ mRNA, while postnatal γδ thymocytes and fetal αβ thymocytes did not (Fig. 1, B and C). We confirmed the expression of IFNγ within ex vivo fetal γδ thymocytes at the protein level (Fig. 1 D), reaching similar levels as found in embryonic day 18 mouse thymocytes (Muñoz-Ruiz et al., 2016), which was associated with their maturation status (Fig. 1 E and Fig. S1 A) and expression of the transcription factor Tbet (Fig. S1 D). Of note, while the level of maturation within fetal γδ thymocytes, despite the high variation, appeared to be higher compared with postnatal γδ thymocytes as assessed by the absence of CD1a expression, this probably does not reflect the relative absence of immature cells as this was not the case when assessed by the presence of CD27, a marker for mature thymocytes (Fig. 1 C and Fig. S1, B and C). More generally, fetal γδ but not αβ thymocytes were highly enriched for "cytokines" (analysis with Database for Annotation, Visualization, and Integrated Discovery [DAVID]: P = 0.00013 for functional annotation "cytokine"). Of note, in addition to TNF, a more general enrichment of members of the TNF superfamily was observed within fetal γδ thymocytes, including TRAIL (TNFSF10) and RANKL (TNFSF11; Dokouhaki et al., 2013; Roberts et al., 2012; Fig. 1 B and Table S1). Among highly enriched genes were also the cytokine CSF1 (M-CSF; Mamedov et al., 2018), the wound-healing associated cytokine amphiregulin (Guo et al., 2018; Krishnan et al., 2018), and the chemokines CCL4 and XCL1 (Table S1). At late gestation, mouse thymocytes (Vγ6$^+$) are programmed to make IL17 (Haas et al., 2012). We could not detect RNA transcripts of any of the IL17 members in human fetal γδ thymocytes. However, a range of genes described to have a role in IL17 production in γδ T cells were enriched within fetal γδ thymocytes: MAF, RORC (RORG), TGFBR3 and SMAD, IL23R and IL1R, BLK, and CCR6 (Haas et al., 2009; Do et al., 2010; Laird et al., 2010; Zuberbuehler et al., 2019; Table S1).

A striking observation was the high expression of cytotoxic granule-associated molecules within fetal γδ thymocytes, including several granzymes (Fig. 1, B–D). Protein expression of granzyme A was, like IFNγ, associated with maturation status (Fig. 1 E and Fig. S1 A). Furthermore, fetal γδ thymocytes expressed high levels of the transcription factor promyelocytic leukemia zinc finger (PLZF; also known as zinc finger and BTB domain containing 16 [ZBTB16]), a key "innate lymphocyte" regulator (Savage et al., 2008; Kovalovsky et al., 2008; Kreslavsky et al., 2009; Fig. 1, B and C), and showed enriched expression for receptors of innate cytokines: IL1R1, IL1RL1 (ST2, the receptor for IL-33), IL18RAP/IL18R1, and IL23R (Fig. 1 B and Table S1).

In summary, fetal γδ thymocytes express high levels of the innate lymphocyte transcription factor PLZF and show an effector functional program (e.g., IFNγ and granzymes) and high expression of receptors for innate cytokines compatible with mature γδ T cells able to respond rapidly in the periphery after leaving the thymus.

Human fetal γδ thymocytes express invariant germline-encoded CDR3γ and CDR3δ

Postnatal γδ thymocytes showed high expression levels of the TdT enzyme (also known as DNA nucleotidylexotransferase [DNTT]), while fetal γδ thymocytes expressed this enzyme only

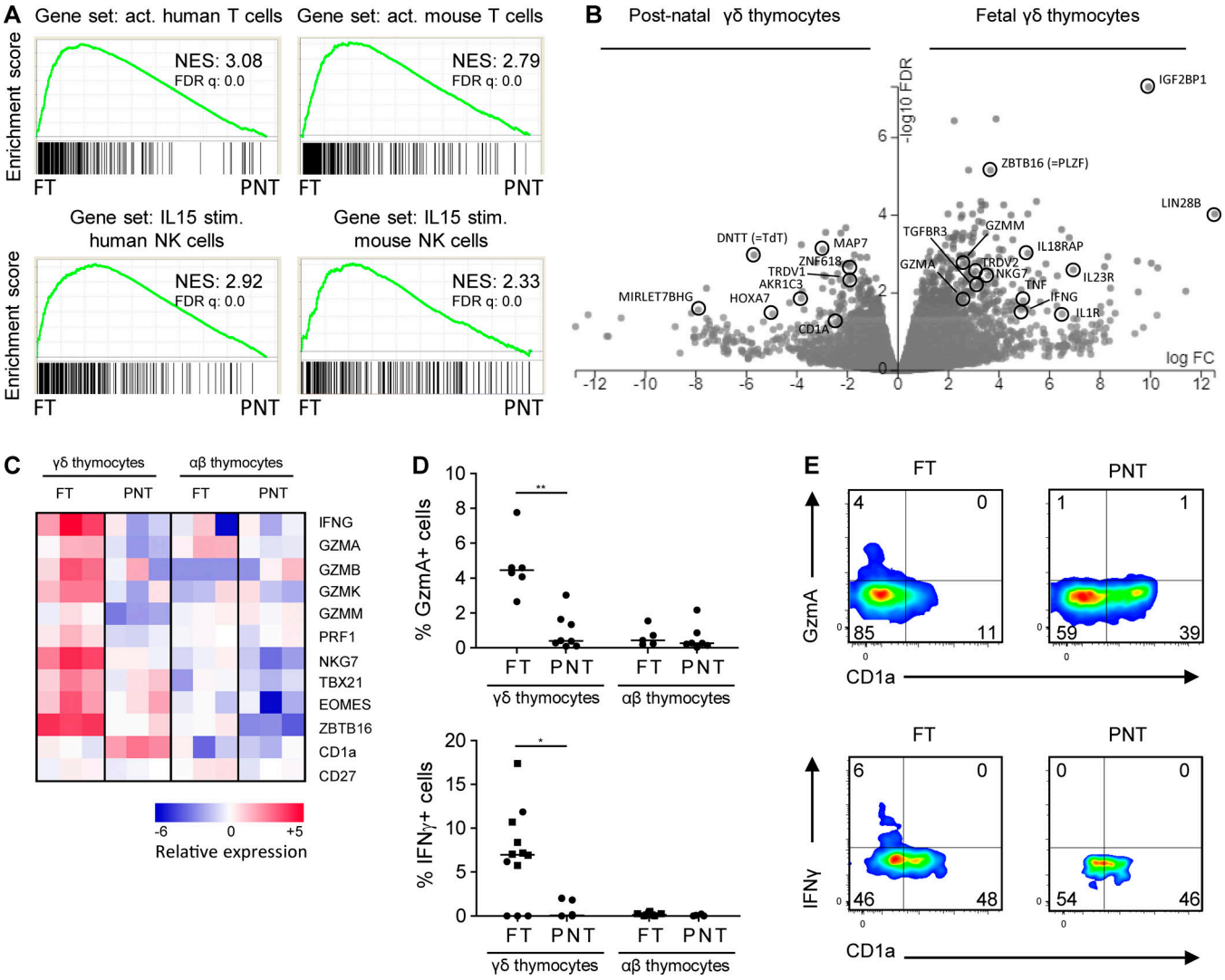

Figure 1. **Fetal γδ thymocytes express programmed effector functions. (A)** γδ thymocytes (without the Vγ9Vδ2 subset) were sorted from FT (n = 3) or PNT (n = 3) samples, and gene expression profiles were determined by RNAseq. GSEA plots based on the RNAseq dataset of FT versus PNT γδ thymocytes with the gene sets of activated (act.; versus naive) human (GSE28726) and mouse (GSE10239) T cells (top) and the gene sets of IL-15–stimulated (stim.; versus unstimulated) human (GSE22886) and mouse (GSE7764) NK cells (bottom). Gene sets are from the C7 immunological gene signature from the MSigDB. **(B)** Volcano plot illustrating differentially expressed genes between FT and PNT γδ thymocytes. **(C)** Heatmap of selected genes in FT and PNT γδ and αβ thymocytes. **(D)** Flow cytometry analysis of granzyme A (top) and IFNγ (bottom) expression by FT and PNT γδ and αβ thymocytes. Each symbol represents an individual donor: square symbols indicate CyToF data, and round symbols for γδ thymocytes indicate γδ thymocytes without the Vγ9Vδ2 subset. Horizontal lines indicate the median, and data were analyzed by Mann Whitney U test. *, P < 0.05; **, P < 0.01. **(E)** Flow cytometry plots of FT and PNT γδ thymocytes (without the Vγ9Vδ2 subset) illustrating the granzyme A$^+$ cells within CD1a$^-$ cells (top) and IFNγ$^+$ cells within CD1a$^-$ cells (bottom); data in the top and bottom panels are obtained from different subjects. The top panels are representative of five (FT) and six (PNT) independent experiments. The bottom panels are representative of one (FT) and seven (PNT) independent experiments. NES, normalized enrichment score.

poorly (Fig. 1 B). Since TdT is essential for CDR3 variability by adding randomly N nucleotides during DNA recombination, we assessed the impact of this differential expression on the CDR3γ and CDR3δ repertoire. First, we performed flow cytometry with Vγ- and Vδ-specific antibodies and found that the FT showed a striking enrichment of the postnatally minor Vγ9$^-$Vδ2$^+$ subset (Fig. 2 A; Morita et al., 1994; Vermijlen et al., 2010; Davey et al., 2018). Analysis at the mRNA level of V gene segment usage (TRGV and TRDV) in the CDR3γ and CDR3δ repertoire showed usage of all functional TRGV genes and of the nonfunctional (Zhang et al., 1994) TRGV10 gene segment and confirmed the increased usage of the TRDV2 gene segment within fetal γδ thymocytes, while TRDV1 was the main TRDV gene segment used in the postnatal γδ thymocytes (Fig. 2 B). Analyzing the CDR3 clonotypes revealed that postnatal thymocytes show a polyclonal repertoire (Fig. 2, C and D), as recently described (Kallemeijn et al., 2018; Di Lorenzo et al., 2019). In contrast, however, fetal γδ thymocytes displayed an oligoclonal repertoire (Fig. 2, C and D), especially the CDR3γ. Indeed, the first 10 most abundant CDR3γ clonotypes accounted for about half of all the fetal γδ thymocyte CDR3γ repertoire (Fig. 2 D). Consistent with the low expression of the TdT enzyme in fetal γδ thymocytes

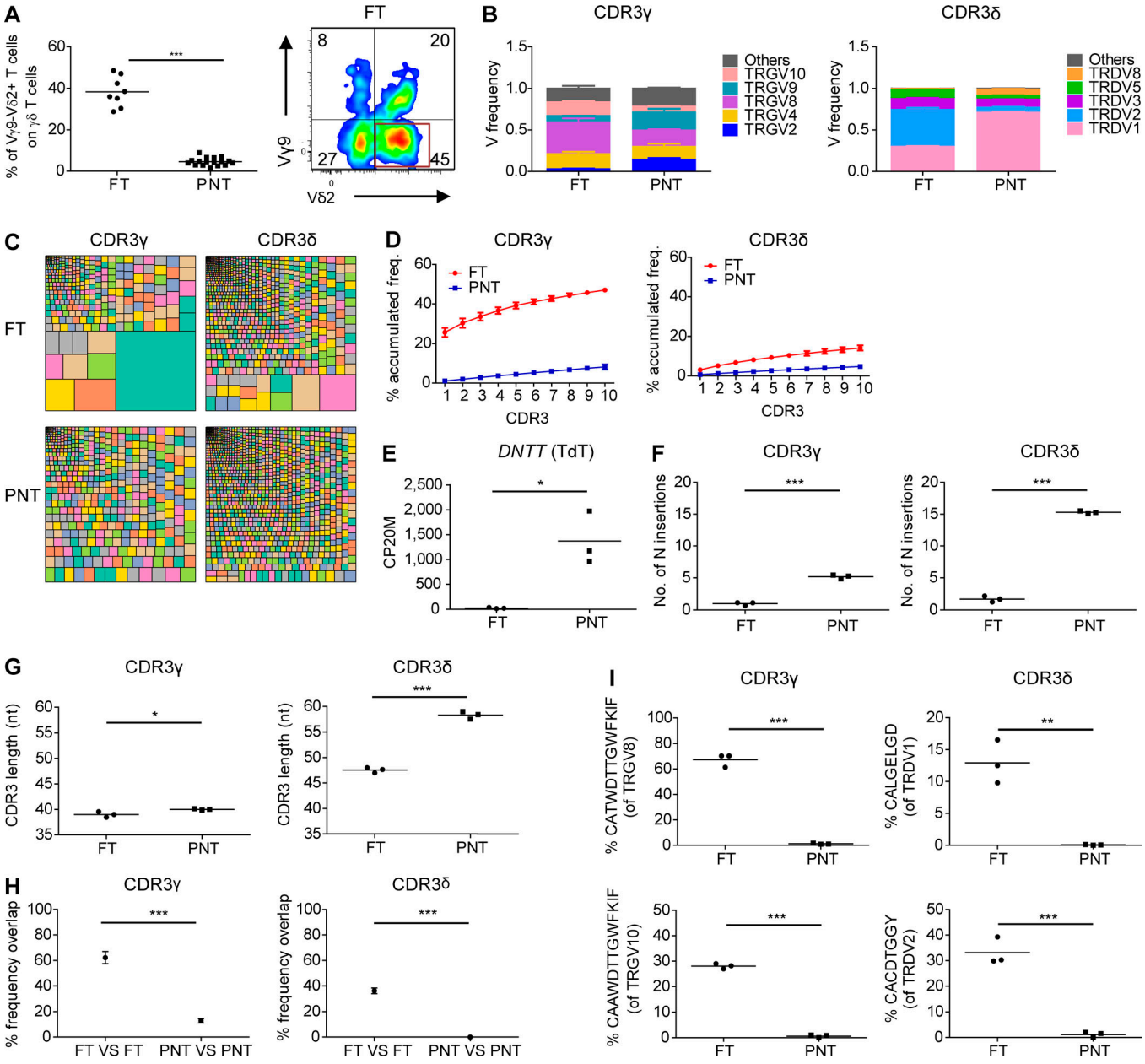

Figure 2. **Human fetal γδ thymocytes express invariant germline-encoded CDR3γ and CDR3δ repertoires. (A)** Flow cytometry analysis of the expression of Vγ9⁻Vδ2⁺ γδ T cell subset in FT and PNT γδ thymocytes (left); representative flow cytometry plot of fetal γδ thymocytes (right). **(B)** HTS analysis of the V gene segment usage TRGV (left) and TRDV (right) in FT and PNT γδ thymocytes. TRG "Others" groups: TRGV1-TRGV3, TRGV5, TRGV5P, TRGV7, and TRGV11 variable chains; TRD "Others" groups: TRDV4, TRDV6, and TRDV7 variable chains. **(C)** Tree map representations of the CDR3γ and CDR3δ repertoires of FT and PNT γδ thymocytes (colors used are random; no correspondence between graphs). Representative of three independent experiments. **(D)** Accumulated frequencies (freq.) of the 10 most abundant clonotypes in CDR3γ and CDR3δ repertoires of γδ thymocytes in FT and PNT. **(E)** Analysis of the "counts per 20 million" (CP20M; RNAseq data) of the DNTT gene of γδ thymocytes in FT and PNT. **(F and G)** Mean number of N insertions (F) and CDR3 length (G; number of nucleotides) in CDR3γ and CDR3δ repertoires of γδ thymocytes in FT and PNT. **(H)** Overlap analysis showing the percentage of shared CDR3γ and CDR3δ clonotypes among three FT γδ thymocytes and among three PNT γδ thymocytes. **(I)** Percentage of particular clonotype amino acid sequences in CDR3γ and CDR3δ repertoires in FT and PNT γδ thymocytes. Each symbol (A, E–G, and I) represents an individual donor. Graphs show the means ± SEM (B, D, and H) or the mean (A, E–G, and I). Data were analyzed by Student's *t* test; *, P < 0.05; **, P < 0.01; ***, P < 0.001. *n* = 8 (FT) and 17 (PNT; A) or *n* = 3 (FT and PNT; B–I).

(Fig. 1 B and Fig. 2 E), we found only a very low number of N insertions within the CDR3γ and CDR3δ (Fig. 2 F and Fig. S2 A). In contrast, the number of N insertions was high in postnatal thymocytes, with the CDR3δ showing a mean number of N insertions of 15, which was much higher than CDR3γ but also than CDR3α and CDR3β (Fig. 2 F and Fig. S3 A). The low level of N insertions in fetal γδ thymocytes resulted in an expected shorter CDR3δ length, which was also seen for CDR3α and CDR3β (Fig. 2 G and Fig. S3 B). Surprisingly, this was not the case for CDR3γ, which was likely due to a difference in TRGJ usage between fetal and postnatal γδ thymocytes: fetal γδ thymocytes were enriched for TRGJP1, which contains 4 nt more than TRGJ1,

the most abundant TRGJ in postnatal thymocytes (Fig. S2 C), coinciding with the difference in N insertions (Fig. 2 F). This preferential TRGJP1 usage was most striking with TRGV8 and TRGV10 (Fig. S2 D), prevalent TRGV gene segments within fetal γδ thymocytes (Fig. 2 B). There was also a different TRDJ usage between fetal and postnatal thymocytes: a significant proportion of fetal γδ thymocyte CDR3δ used TRDJ2 and TRDJ3, while these TRDJs were only minimally present in postnatal thymocytes, where the vast majority used TRDJ1 (Fig. S2 C). This was observed with every TRDV (Fig. S2 D). Note that while the mean CDR3α and CDR3β lengths from αβ thymocytes were similar (Fig. S3 B), the CDR3γ length of γδ thymocytes was significantly smaller than the CDR3δ length (Fig. 2 G). Such a differential CDR3 length between the γ and δ chain has been described previously and is also found between the heavy and light chain of the B cell receptor/antibodies (Rock et al., 1994; Chien and Konigshofer, 2007).

We found that the repertoire of fetal γδ thymocytes was highly shared, i.e., exactly the same clonotypes were used in fetal γδ thymocytes derived from different subjects (Fig. 2 H). Investigating this further, we detected a striking enrichment of particular clonotype sequences that were completely germline encoded (i.e., no N and P nucleotides): TRGV8-TRJP1 CATWDTTGWFKIF, TRVG10-TRJP1 CAAWDTTGWFKIF, TRDV2-TRDD3 CACDTGGY, and TRDV1-TRDD3 CALGELGD (Fig. 2 I).

In summary, fetal γδ thymocytes show clearly a distinct γδ TCR repertoire possessing CDR3 with low N insertions, coinciding with low TdT expression, resulting in a highly shared repertoire that is strikingly enriched for particular invariant CDR3 sequences.

The capacity to generate γδ T cells with programmed effector functions, low TdT expression, and invariant CDR3γ and CDR3δ is a property of fetal HSPCs

The first wave of mouse γδ T thymocytes (possessing an invariant Vγ5Vδ1 TCR) can be generated in a fetal thymic organ culture system only when HSPCs of fetal origin, and not adult, are used (Ikuta et al., 1990; Havran and Allison, 1990). We wondered whether the unique properties of fetal γδ thymocytes described above (programmed function, invariant CDR3) could be due to differences in HSPCs present early versus later in life. To address this, we used the in vitro OP9DL1 co-cultures that are efficient in generating human γδ T cells starting with CD34$^+$ HSPCs (Van Coppernolle et al., 2009). Thus, we generated γδ T cells in vitro starting with CD34$^+$ HSPCs derived from several sources: fetal liver (FL; 15–21 wk gestation), fetal blood (FB; 24–31 wk gestation), CB (>37 wk gestation), and mobilized adult blood (AB; >18 yr).

Gene expression profiling and gene set enrichment analysis (GSEA) revealed that FL-derived γδ T cells clearly shared their gene expression profile with fetal γδ thymocytes, while AB-derived γδ T cells shared their gene expression profile with postnatal γδ thymocytes (Fig. 3 A). In line with this, FL-derived γδ T cells shared their gene expression profile with activated T cells and IL15-stimulated NK cells (Fig. 3 B). FL-derived γδ T cells, in contrast to AB-derived γδ T cells, were highly enriched for IFNγ, TNFα, secretory granule-associated molecules, CCL4, TGFBR3, PLZF (ZBTB16), and IL18RAP (Fig. 3 C). On the other hand, TdT (DNTT) showed high expression in AB-derived γδ T cells (Fig. 3 C). Thus FL-derived γδ T cells replicated the functional program observed in fetal γδ thymocytes.

Analysis of the Vδ and Vγ expression on the cell surface by flow cytometry revealed that fetal HSPCs (FL and FB) are very efficient in the generation of Vδ2$^+$ cells (Fig. 4, A–C), which was confirmed by V gene segment usage analysis by high-throughput sequencing (HTS; Fig. 4 D). Thus, as observed in ex vivo fetal versus postnatal γδ thymocytes (Fig. 1 B and Fig. 2 B), FL/FB-derived γδ T cells and CB/AB-derived γδ T cells were enriched for TRDV2 and TRDV1, respectively (Fig. 3 C and Fig. 4 D). The CDR3γ and CDR3δ repertoires in fetal HSPC OP9DL1 cultures were more oligoclonal than the repertoires derived from OP9DL1 cultures with HSPC sources of later life (CB and AB; Fig. 5, A and B) and expressed low TdT levels (Fig. 5 C), resulting in a low number of N insertions (Fig. 5 D), again as observed ex vivo in fetal versus postnatal γδ thymocytes (Fig. 2, C–F). In comparison to the CDR3 repertoire of CB/AB-derived γδ T cells, the CDR3 repertoire of FL/FB-derived γδ T cells was highly shared and also showed high sharing with the ex vivo fetal γδ thymocytes (Fig. 5 E). Strikingly, FL/FB-derived, but not CB/AB-derived, γδ T cells were efficient in the generation of the invariant germline-encoded CDR3 sequences TRGV8-TRJP1 CATWDTTGWFKIF, TRDV2-TRDD3 CACDTGGY, and TRDV1-TRDD3 CALGELGD (Fig. 5 F), which are also enriched in fetal γδ thymocytes ex vivo (Fig. 2 I).

In summary, fetal HSPC-derived γδ T cells (using the in vitro T cell development system OP9DL1) share with ex vivo fetal γδ thymoctyes: (i) a functional effector program; (ii) low TdT expression; and (iii) invariant germline-encoded CDR3 sequences, indicating that stem cell-autonomous mechanisms are underlying the generation of the programmed and invariant human γδ thymocytes.

The invariant germline-encoded CDR3γ and CDR3δ are generated independently of functional TCR expression

We wondered whether a selection mechanism is involved in the observed invariant sequences that are prevalent in fetal γδ thymocytes and dependent on fetal HSPCs. We therefore analyzed the preselection γδ TCR repertoire of (i) sorted CD3neg T cell progenitors from the OP9DL1 cultures and (ii) TRGV10-containing CDR3 sequences, which cannot express a TCR at the cell membrane. Indeed, TRGV10 is expressed at the RNA level but cannot be further translated because of the absence of splicing of the leader intron that leads to the generation of a stop codon (Zhang et al., 1994; and confirmed by the analysis of our HTS data: Fig. S4). By comparing the CDR3 repertoire of sorted γδ T cells from OP9DL1 cultures with that of sorted progenitors, we found that already at the progenitor level, the rearranged CDR3 sequences of FL and FB HSPC cultures show low N insertions and are highly enriched for the invariant germline-encode CDR3 sequences TRGV8-TRGJP1 CATWDTTGWFKIF, TRDV2-TRDD3 CACDTGGY, and TRDV1-TRDD3 CALGELGD (Fig. 5, D and F). Our HTS strategy based on template-switch cDNA generation allowed us to generate CDR3 sequences containing the nonfunctional VγIII member TRGV10 (Zhang et al.,

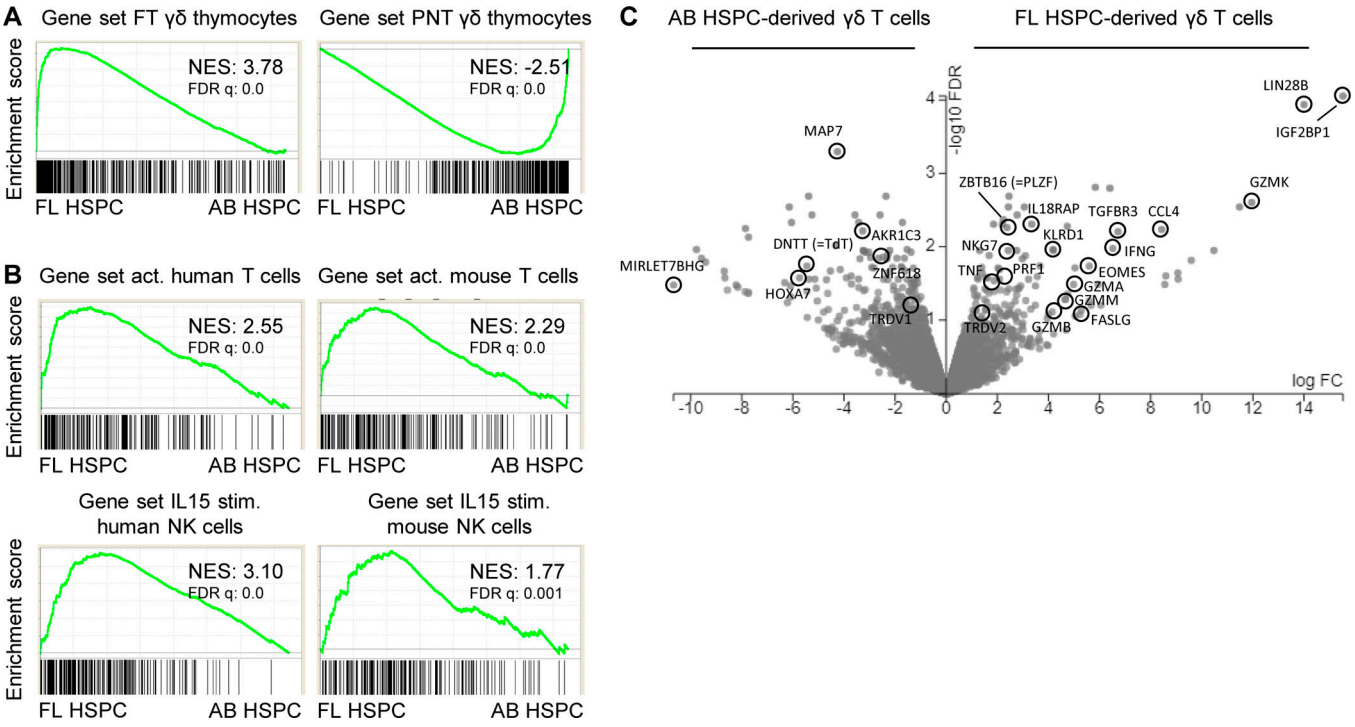

Figure 3. **Human fetal HSPC-derived γδ T cells share a functional transcriptional profile with fetal γδ thymocytes.** γδ T cells were sorted from OP9DL1 cultures either derived from FL HSPCs (n = 3) or AB HSPCs (n = 3), and gene expression profiles were determined by RNAseq. **(A)** GSEA plots quantifying the shared profile of FL-derived and AB-derived γδ T cells with FT and PNT thymocytes, respectively. **(B)** GSEA plots quantifying the shared profile of FL-derived and AB-derived γδ T cells with activated (act.; versus naive) human (GSE28726) and mouse (GSE10239) T cells (top) and with IL-15–stimulated (stim.; versus unstimulated) human (GSE22886) and mouse (GSE7764) NK cells (bottom). Gene sets are from the C7 immunological gene signature from the MSigDB. **(C)** Volcano plot illustrating differentially expressed genes between FL- and AB-derived γδ T cells. NES, normalized enrichment score.

1994; in contrast to using specific primers against the VγI [members TRGV2, 3, 4, 5, and 8] and VγII [member TRGV9]; Ravens et al., 2017; Davey et al., 2017, 2018). We found that TRGV10-containing CDR3 sequences were strikingly enriched for the TRGV10-TRGJP1 CAAWDTTGWFKIF sequence both in ex vivo fetal γδ thymocytes (Fig. 2 I) and FL/FB-derived γδ T cells (Fig. 5 F). As expected, this TRGV10-associated sequence was also already enriched at the progenitor level of FL/FB OP9DL1 cultures (Fig. 5 F). Thus, we conclude that the high frequency of invariant germline-encoded sequences is not caused by a selection of these sequences among many other rearranged CDR3 sequences but is intrinsically determined at the level of the HSPC/γδ progenitor.

The V, J, and D gene segments composing the invariant germline-encoded CDR3γ and CDR3δ contain short homology repeats

As the high enrichment of invariant CDR3γ and CDR3δ within the FT and within fetal HSPC-derived γδ T cells appears not to be due to a selection process involving the TCR, we investigated alternative mechanisms. While the low expression of TdT (Fig. 2 E and Fig. 5 C) certainly contributes to a lower diversity within the CDR3, there are still a variety of recombinations possible involving different V and/or (D)J regions, with different degrees of removal of nucleotides at their ends before joining. This variation can be further increased by the addition of P nucleotides. Thus, despite this variation potential, particular sequences or motifs showed a striking enrichment (Fig. 2 I and Fig. 5 F). Inspired by previous work in the mouse model (Itohara et al., 1993; Asarnow et al., 1993; Zhang et al., 1995), we discovered the presence of short homology repeats located at the 3′ end of the TRGV8/TRDV1/TRDV2 sequences and 5′ end of the TRGJP1/TRDD3 sequences (Fig. 6 A). These short homology repeats likely contribute to the enrichment of the observed invariant CDR3 sequences (Fig. 6, B and C). Such a motif was even observed for TRGV10 (to recombine with TRGJP1), which cannot generate a functional Vγ chain (Zhang et al., 1994; Fig. 6 A). Note that a 1-nt difference between TRDV1 and TRDV2 of the location of the short homology repeat resulted in a completely different invariant CDR3 sequence because of a different open-reading frame usage of the TRDD3 gene segment (Fig. 6 C). Thus, it appears that the absence of N nucleotides allows the recombination based on short homology repeats, thus generating the invariant germline-encoded sequences in fetal γδ thymocytes and FL/FB-derived γδ T cells: TRGV8-TRGJP1 CATWDTTGWFKIF, TRGV10-TRGJP1 CAAWDTTGWFKIF, TRDV2-TRDD3 CACDTGGY, and TRDV1-TRDD3 CALGELGD.

Lin28b induces an effector program, inhibits TdT expression, and enhances the formation of germline-encoded invariant CDR3γ and CDR3δ sequences

Both in ex vivo fetal γδ thymocytes (versus postnatal γδ thymocytes; Fig. 1 B) and in FL HSPC-derived γδ T cells (versus AB HSPC-derived γδ T cells; Fig. 3 C), the expression of the RNA-

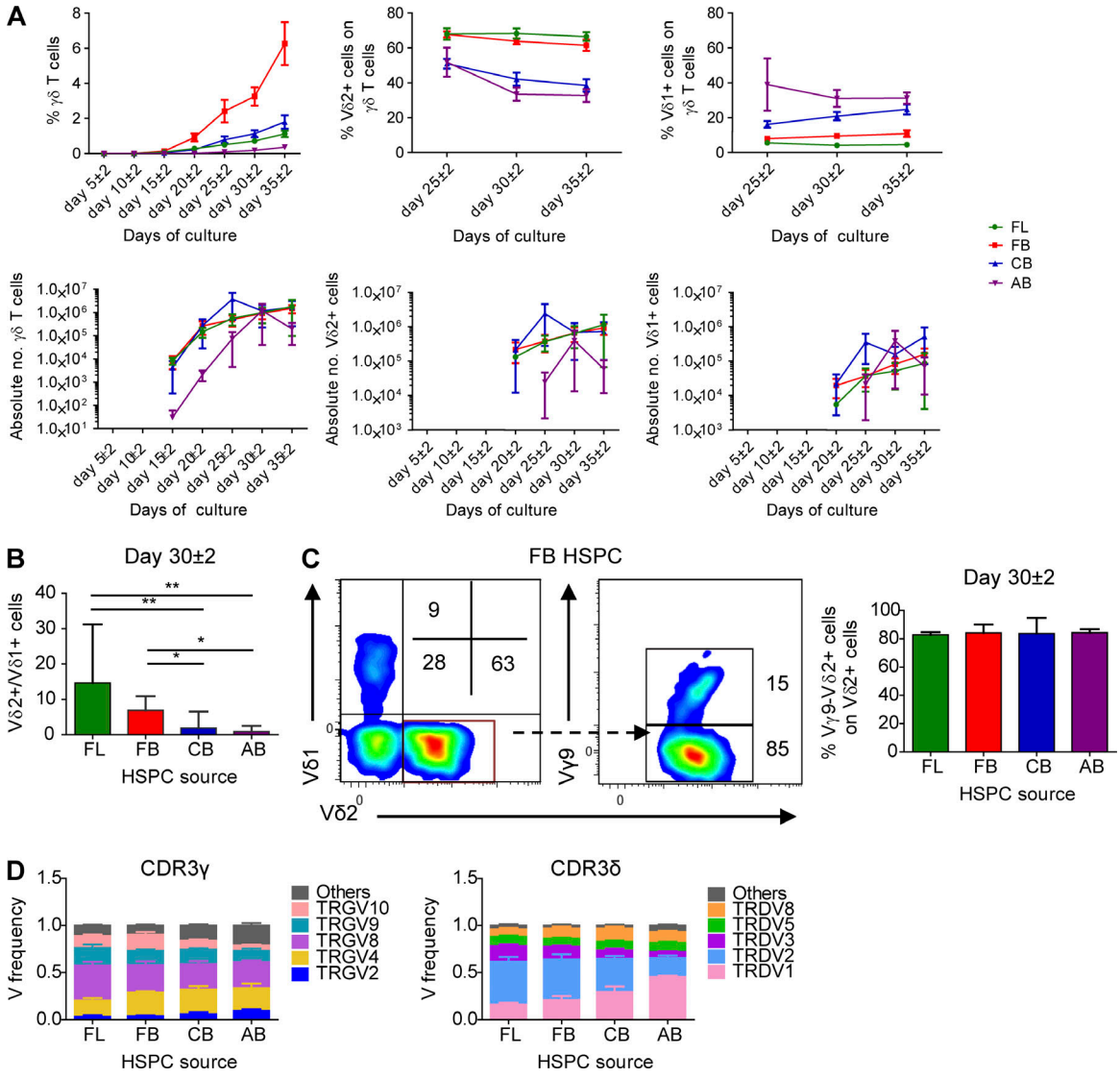

Figure 4. **Human fetal HSPCs efficiently generate Vγ9⁻Vδ2⁺ γδ T cells. (A)** Kinetics of the percentage of γδ T cells (of CD7⁺ cells), Vδ2⁺, and Vδ1⁺ γδ T cells (top) and of the absolute number (bottom) analyzed by flow cytometry and derived from FL, FB, CB, and AB HSPCs during co-culture with OP9DL1 cells. For each time point, *n* ranges from 2 to 3 (FL), 6 to 9 (FB), 7 to 11 (CB), and 3 to 4 (AB). **(B)** Ratio between Vδ2⁺ versus Vδ1⁺ γδ T cells at day 30 ± 2 of OP9DL1 co-culture (*n* = 3, 9, 11, and 4, respectively, for FL-, FB-, CB-, and AB-derived HSPCs). **(C)** Flow cytometry analysis of the expression of Vδ2 and Vδ1 chains of γδ T cells derived from FB HSPCs and of the expression of the Vδ9 chain on the Vδ2⁺ γδ T cells at day 30 ± 2. Numbers indicate the percentage of the corresponding population. Data are representative of 11 independent experiments. On the right, percentage of the Vγ9-Vδ2⁺ γδ T cell subset (gated on Vδ2⁺ γδ T cells) from FL, FB, CB, and AB HSPCs at day 30 ± 2 of OP9-DL1 co-culture (*n* = 3, 9, 11, and 4, respectively, for FL, FB, CB, and AB). **(D)** HTS analysis of the V gene segment usage TRGV (left) and TRDV (right) of sorted γδ T cells derived from FL (*n* = 3), FB (*n* = 4), CB (*n* = 6), and AB (*n* = 3) HSPCs. TRG "Others" groups: TRGV1-TRGV3, TRGV5, TRGV5P, TRGV7, and TRGV11 variable chains; TRD "Others" groups: TRDV4, TRDV6, and TRDV7 variable chains. Graphs show the means ± SEM (A and D) or the medians ± range (B and C). Data were analyzed by Kruskal-Wallis ANOVA followed by Dunn's multiple comparison test; *, $P < 0.05$; **, $P < 0.01$.

binding protein Lin28b was highly enriched, and MIRLET7B was highly depleted. Lin28b can block the bioprocessing of let-7 family microRNAs (miRNAs; Jiang and Baltimore, 2016; Rowe et al., 2016), providing an explanation of why the MIRLET7B host gene (MIRLET7HG) transcript is highly enriched within postnatal γδ thymocytes and AB-derived γδ T cells (Fig. 1 B and Fig. 3 C). As this RNA-binding protein has been described to be involved in murine innate-like lymphopoiesis (Yuan et al., 2012; Jiang and Baltimore, 2016), we wondered whether Lin28b is involved in the programmed effector functions, low TdT expression, and/or invariant CDR3 sequences that we observed in fetal γδ thymocytes and FL-derived γδ T cells. To test this hypothesis, we transduced CB HSPCs to express the human *LIN28B* gene and compared the γδ T cells derived from the *LIN28B* versus control OP9DL1 cultures. Lin28b overexpression resulted in a shared gene expression profile with FL-derived γδ T cells (Fig. 7 A), and in line with this, with activated T cells and IL15-stimulated NK cells (Fig. 7 B), as illustrated by an increase in the expression of effector molecules and the increased expression of PLZF (ZBTB16) and

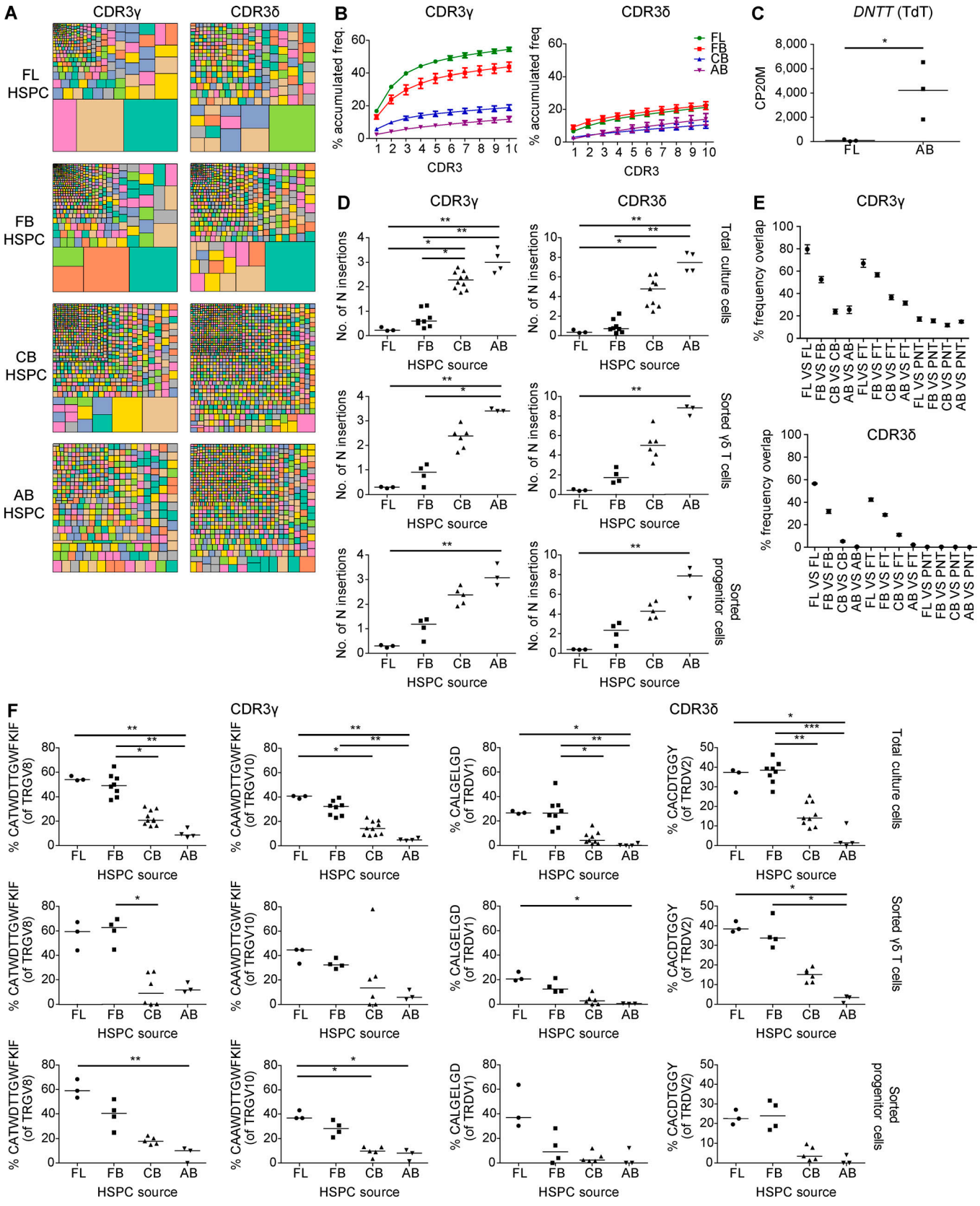

Figure 5. **Human fetal HSPCs efficiently generate invariant CDR3γ and CDR3δ sequences. (A)** Tree map representations of the CDR3γ and CDR3δ repertoires of OPDL1 cultures derived from FL, FB, CB, and AB HSPCs (colors in the tree maps are random; no correspondence between graphs). Graphs are representative of 3 (FL), 8 (FB), 10 (CB CDR3γ), 9 (CB CDR3δ), and 4 (AB) independent experiments. **(B)** Accumulated frequencies (freq.) of the 10 most abundant clonotypes of the CDR3γ and CDR3δ repertoire derived from total cells. FL (n = 3), FB (n = 8), CB (n = 10 for CDR3γ and 9 for CDR3δ), and AB (n = 4).

(C) CP20M of the RNAseq data of DNTT (TdT) of γδ T cells derived from FL and AB HSPCs. **(D)** Mean number of N insertions in CDR3γ and CDR3δ repertoires of total cells, sorted γδ T cells, and sorted progenitor cells derived from FL, FB, CB, and AB HSPCs after co-culture with OP9DL1 cells. **(E)** Overlap analysis showing the percentage of shared CDR3γ and CDR3δ clonotypes among three FL, four FB, six CB, and three AB sorted γδ T cells derived from HSPCs and among these groups with three FT and three PNT thymus nonVγ9Vδ2 sorted γδ thymocytes. **(F)** Percentage of particular CDR3 clonotype amino acid sequences present in total cells, sorted γδ T cells, and sorted progenitor cells derived from FL, FB, CB, and AB HSPCs. Each symbol (C, D, and F) represents an individual donor. Graphs show the means ± SEM (B and E). Data were analyzed by Student's *t* test (C) and Kruskal-Wallis ANOVA followed by Dunn's multiple comparison test (D and F); *, P < 0.05; **, P < 0.01; ***, P < 0.001.

IGF2BP1 (another RNA-binding protein; Fig. S5 A). This was associated at the TCR/CDR3 level with a higher TRDV2/TRDV1 ratio (Fig. 7 C), increased oligoclonality (Fig. S5 B), a striking inhibition of TdT expression (Fig. 7 D) resulting in decreased N insertions (Fig. 7 E), and increased sharing (Fig. 7 F). Importantly, the overexpression of Lin28b led as well to an increased sharing of the CDR3 repertoire with FL/FB-derived γδ T cells (Fig. 7 F) and to increased levels of the germline-encoded invariant sequences (Fig. 7 G and Fig. S5 C). Note that, as before, the decreased level of N insertions and increased level of invariant CDR3 sequences was already observed at the progenitor level (Fig. 7 E and G; and Fig. S5 C).

We conclude that the RNA-binding protein Lin28b is a major determinant in the HSPC-dependent generation of human fetal invariant and programmed effector γδ thymocytes.

Discussion

In this study we provide a detailed description of the differences between human fetal and postnatal γδ thymocytes with regard to programmed effector function and invariant CDR3 sequences. Furthermore, we demonstrated that these differences are HSPC-dependent and are mediated to a major extent by the RNA-binding protein Lin28b.

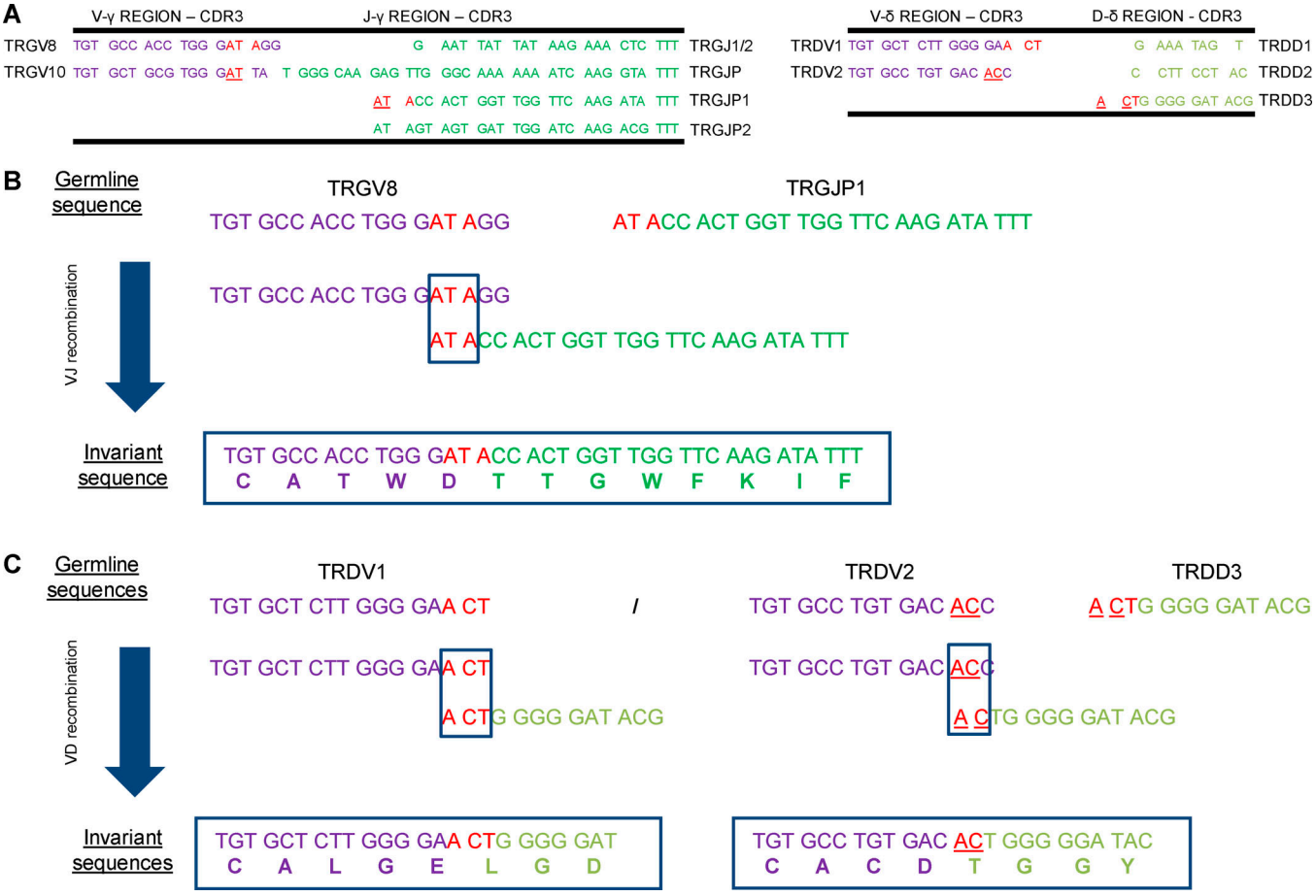

Figure 6. **Short homology repeats at the VDJ junctions. (A)** Left, table showing the nucleotide sequences of the variable gene segments TRGV8 and TRGV10 (3′ ends, CDR3) and of the five joining gene segments TRGJ (J1/J2, JP, JP1, and JP2; 5′ ends, CDR3). Right, table showing the nucleotide sequences of the variable gene segments TRDV1 and TRDV2 and of the three diversity gene segments TRDD (D1, D2, D3). Short homology repeats are shown in red or in red and underlined. **(B)** Recombination using short homology repeats between TRGV8 and TRGJP1. Overlapping nucleotides are shown in red. **(C)** Recombination using short homology repeats between TRDV1 and TRDD3 and between TRDV2 and TRDD3. Overlapping nucleotides are shown in red (TRDV1-TRDD3) and in underlined red (TRDV2-TRDD3).

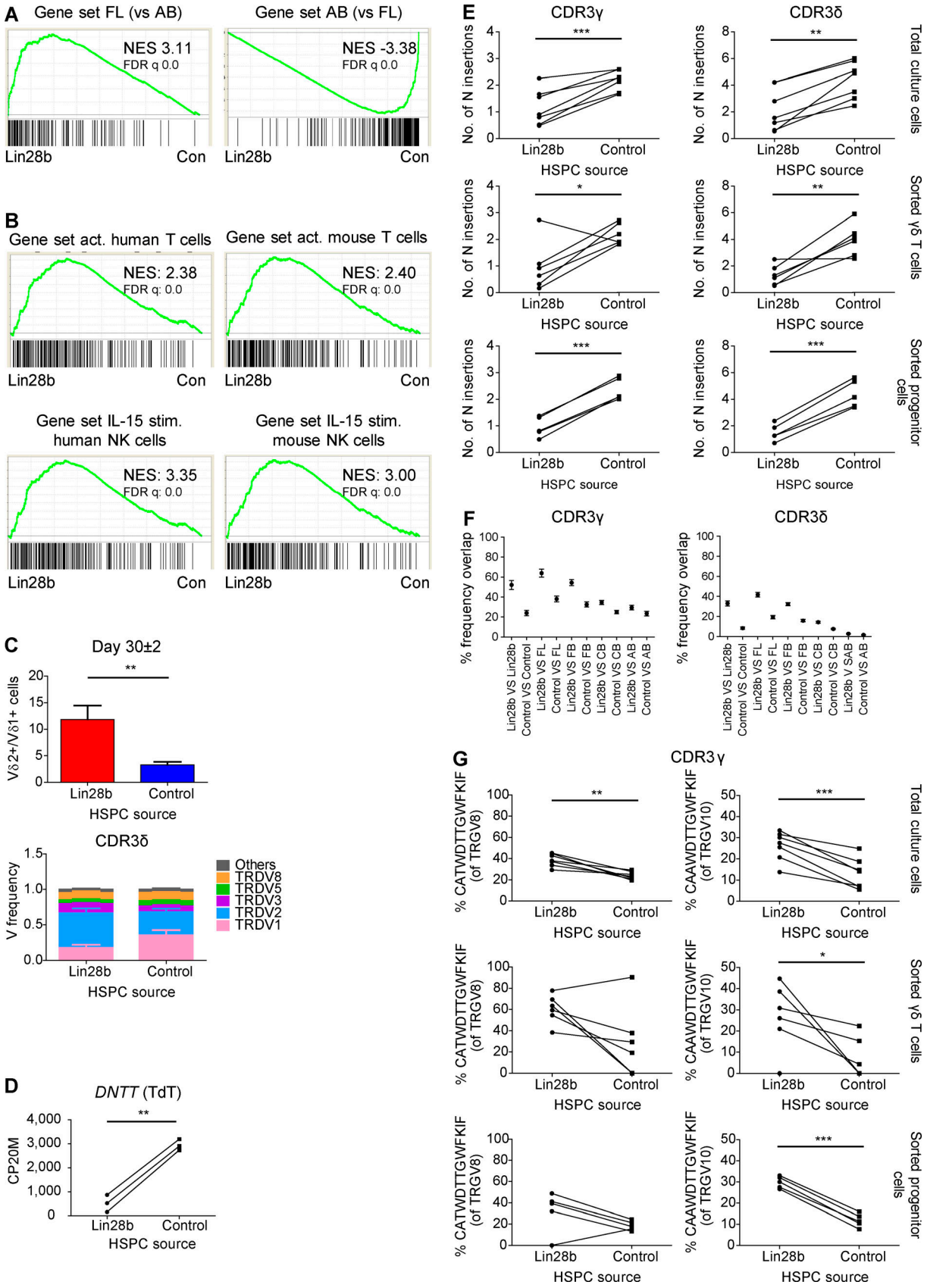

Figure 7. **Lin28b induces an effector program, inhibits TdT expression, and enhances the formation of germline-encoded invariant CDR3γ and CDR3δ sequences. (A)** γδ T cells were sorted from OP9DL1 cultures either derived from Lin28b-transduced CB HSPCs (Lin28b; *n* = 3) or control-transduced CB HSPCs (Con.; *n* = 3). GSEA plots based on RNAseq data quantifying the shared profiles of Lin28b-derived versus control-derived γδ T cells with FL and AB HSPC-

derived γδ T cells as gene sets. **(B)** GSEA plots quantifying the shared profile of Lin28b- versus control-transduced CB HSPC-derived γδ T cells with activated (act.; versus naive) human (GSE28726) and mouse (GSE10239) T cells (top) and with IL-15–stimulated (stim.; versus unstimulated) human (GSE22886) and mouse (GSE7764) NK cells (bottom). Gene sets are from the C7 immunological gene signature from the MSigDB. NES, normalized enrichment score. **(C)** Top, ratio between $V\delta2^+$ and $V\delta1^+$ γδ T cells derived from Lin28b-transduced CB HSPCs (Lin28b) and from control-transduced CB HSPCs (control) at day 30 ± 2 of OP9DL1 co-culture as determined by flow cytometry (n = 9 for Lin28b and control). Bottom, HTS analysis of the TRDV usage on sorted γδ T cells from Lin28b- and control-transduced CB HSPCs. "Others" groups: TRDV4, TRDV6, and TRDV7 variable chains (n = 5). **(D)** Paired comparison analysis of the CP20M RNAseq data of DNTT (TdT) expressed in γδ T cells derived from Lin28b- versus control-transduced CB HSPCs. **(E)** Mean number of N insertions in CDR3γ and CDR3δ repertoires of total cells, sorted γδ T cells, and sorted progenitor cells derived from Lin28b- versus control-transduced CB HSPCs. **(F)** Overlap analysis showing the percentage of shared CDR3γ and CDR3δ clonotypes among sorted γδ T cells (n = 6) derived from Lin28b- versus control-transduced CB HSPCs and among these samples with three FL, four FB, six CB, and three AB sorted γδ T cells derived from HSPCs. **(G)** Percentage of particular CDR3 clonotype amino acid sequences present in total cells, sorted γδ T cells, and sorted progenitor cells derived from Lin28b- versus control-transduced CB HSPCs. Lines between symbols link samples from the same subject (D, E, and G). Data are means ± SEM (C and F). Data were analyzed by paired Student's t test; *, $P < 0.05$; **, $P < 0.01$; ***, $P < 0.001$.

Human fetal γδ thymocytes shared gene expression profiles with activated T cells and IL15-stimulated NK cells. Of note, IL15 has been found to play an important role in the development of innate γδ T cells (Vγ5Vδ1) in the mouse FT (De Creus et al., 2002). Human fetal γδ thymocytes expressed high levels of the innate lymphocyte transcription factor PLZF and showed an effector functional program (e.g., IFNγ and granzymes) and high expression of receptors for innate cytokines. Furthermore, we found that this thymic programming is determined at the level of fetal HSPCs. This is in marked contrast with the described bias of human fetal peripheral αβ T cells toward the regulatory T cell lineage to suppress fetal antimaternal immunity (Mold et al., 2008, 2010). However, the fetus also needs to be protected against congenital infections and exposure to pathogens at birth (Kollmann et al., 2017). The γδ functional effector profile programmed within the FT may contribute efficiently to such protection. We have shown previously that upon congenital CMV infection, γδ T cells are expanded in the periphery and express high levels of IFNγ and granzymes (Vermijlen et al., 2010). We here show that this functional program may be established within the FT. Alternatively, such a programmed functional program could serve "nonimmunological" functions in early life, such as body temperature regulation at birth and brain development (Kohlgruber et al., 2018; Ribeiro et al., 2019).

Fetal and postnatal γδ thymocytes clearly differed in their TCR repertoire. While some differences have been described previously (such as the preferred TRDV2 usage in the FT; McVay et al., 1991; Krangel et al., 1990), a main finding in this study was the identification via HTS of highly enriched germline-encoded invariant CDR3 sequences within fetal γδ thymocytes (TRGV8-TRGJP1 CATWDTTGWFKIF, TRGV10-TRGJP1 CAAWDTTGWFKIF, TRDV2-TRDD3 CACDTGGY, and TRDV1-TRDD3 CALGELGD). While the low TdT expression can contribute to a lower CDR3 variability, it cannot explain the prevalence of these particular sequences. Furthermore, our data regarding the nonfunctional (Zhang et al., 1994) TRGV10-TRJP1 CDR3 sequence and CDR3 data derived from T cell progenitors strongly indicate that the high prevalence of these sequences does not depend on a γδ TCR-dependent signal. We rather propose that the presence of short homology repeats at the end of the involved V, D, and J gene segments can dictate the recombination sites. Such short homology repeats have been identified previously in "early" mouse invariant CDR3 sequences (Itohara et al., 1993; Zhang et al., 1995). Importantly, it has been demonstrated (using recombination substrates in a transgenic mouse model) that such repeats have strong effects on the recombination site and that this process is inhibited by the overexpression of TdT (Zhang et al., 1995). Thus, while human and mouse γδ TCR sequences and γδ T cell subsets are usually regarded as highly different, it appears that the mechanism to generate germline-encoded invariant sequences is conserved. Furthermore, it seems that for some recombination events the same short homology repeats are used: "(a)ta" is present at the 3′ end of the human TRGV8/TRGV10 and mouse TRGV5/TRGV6, while "ata" is present at the 5′ end of the human TRGJP1 and mouse TRGJ1 (Itohara et al., 1993). This evolutionary conservation at the level of the generation of the innate γδ mouse and human TCRs parallels the evolutionary conservation of selective γδ T cell responses to butyrophilins and butyrophilin-like proteins (Boyden et al., 2008; Di Marco Barros et al., 2016; Hayday, 2019). The nonfunctional TRGV10-TRGJP1 CAAWDTTGWFKIF CDR3 sequence is very similar to the functional TRGV8-TRJP1 CATWDTTGWFKIF CDR3 sequence, only different in the third amino acid that is encoded by the TRGV gene segment. Of note, while TRGV10 is not functional in humans, the orthologues in other primates studied are functional (Kazen and Adams, 2011). We have found previously a striking enrichment of an invariant Vγ8Vδ1 CMV-reactive TCR in the blood of fetuses and newborns with congenital CMV infection (Vermijlen et al., 2010; Scheper et al., 2013). The CDR3γ of this Vγ8Vδ1 TCR is exactly the same as the one that was found here to be highly enriched in the FT, while the CDR3δ CALGELGD sequence (the part formed by short homology recombination between TRDV1 and TRDD3) present in the CMV-expanded clones was also found here to be highly enriched among FT TRDV1-containing sequences. Furthermore, the FT-enriched TRDV2-TRDD3 CACDTGGY sequence has also been found to be enriched upon congenital CMV infection (Vermijlen et al., 2010). Thus, the short homology repeats contained in the V, D, and J segments forming these germline-encoded invariant sequences may have been evolutionarily selected to ensure antiviral fetal γδ T cells in utero. We propose that these invariant γδ T cells home to peripheral tissues after exiting the thymus and highly expand upon (CMV) infection, explaining their presence within the blood of CMV-infected newborns (Vermijlen et al., 2010). Such an innate establishment of a tissue-associated γδ TCR repertoire from which adaptive expansions can occur has been recently coined "adaptate" biology (Hayday, 2019).

We show here for the first time that Lin28b has a profound influence on the γδ TCR repertoire as well as on the programming of effector functions in γδ thymocytes. The highly conserved RNA-binding protein Lin28b is involved in many biological processes (including development, reprogramming, pluripotency, and metabolism) and can function as an oncogene (Moss et al., 1997; Jiang and Baltimore, 2016; Helsmoortel et al., 2016). Lin28b was highly expressed in ex vivo–derived fetal γδ thymocytes and in in vitro fetal HSPC-derived γδ T cells, while the TdT enzyme was poorly expressed. Overexpression of Lin28b resulted in a striking down-regulation of TdT, which was accompanied by an increased generation in the invariant CDR3 sequences. Thus, it appears that the low TdT expression in fetal γδ thymocytes is the result of an active suppression mechanism mediated by Lin28b. Lin28b can mediate its effects via two main mechanisms: via the down-regulation of members of the let7 miRNA family (that can effect degradation and/or translation of their mRNA targets) or via selectively binding mRNAs to promote their translation (Jiang and Baltimore, 2016). Our data indicate that the let7 pathway is involved, since effects were seen at the mRNA level upon Lin28b overexpression, and MIRLET7BHG was highly enriched in PNTs and AB HSPC-derived γδ T cells. We propose that the active inhibition of TdT expression in developing γδ thymocytes results in no (or very low level of) N nucleotide insertions, allowing the recombination of the short homology repeats to occur, leading to the described generation of invariant TCR sequences. In later life, Lin28b expression is decreased and TdT increased, resulting in the incorporation of N nucleotides, preventing this short homology–mediated recombination. In addition, it is likely that Lin28b also affects the γδ TCR repertoire independently of TdT inhibition, since Lin28b overexpression altered the Vδ gene segment usage (increased Vδ2/Vδ1 ratio).

The effector program (e.g., IFNγ and granzymes) observed in ex vivo fetal γδ thymocytes was HSPC- and Lin28b-dependent. Since these effector molecules do not contain a let7 motif within the 3′ untranslated region of their mRNA sequences (where typically miRNA-binding sites are found; Wells et al., 2017), it is more likely that the Lin28b/let7-dependency is indirect. One possibility is via the innate lymphocyte transcription factor PLZF (ZBTB16), which was highly expressed by ex vivo fetal γδ thymocytes and fetal HSCP-derived γδ T cells and showed increased expression upon Lin28b overexpression. Indeed, PLZF has been shown to be a target of let7 miRNA (Pobezinsky et al., 2015) and to promote the development of mouse innate γδ T cells (Kreslavsky et al., 2009). Also, the RNA-binding protein IGFBP1 (highly prevalent in ex vivo fetal γδ thymocytes and fetal HSPC-derived γδ T cells and increased upon Lin28b expression) is a let7 target (Boyerinas et al., 2008). Interestingly, IGFBP1 has been recently shown to be involved in the generation of human fetal hemoglobin in fetal HSPC-derived erythroblasts (de Vasconcellos et al., 2017). Finally, in contrast to our observations in γδ T cells, Lin28b promotes the generation of regulatory T cells in human peripheral fetal αβ T cells (Bronevetsky et al., 2016), thus highlighting a differential effect of the same RNA-binding protein in the γδ versus αβ T cell lineage. More generally, our study identifies evolutionarily conserved mechanisms in the ontogeny of γδ T cells in humans, and the insights provided can contribute to a better understanding of the immune response toward infectious diseases occurring during fetal life versus adult life (Kollmann et al., 2017; Kan et al., 2016).

Materials and methods

Human cell material

FT (n = 8) and FL (n = 3) samples (15–21 wk gestation) were obtained with approval of the Centralized Institutional Research Board of the Singapore Health Services in Singapore. PNT (n = 17; 4 mo–9 yr) samples and mobilized peripheral blood samples of adult donors (n = 4; >18 yr) were obtained with approval of the Medical Ethical Commission of the Ghent University Hospital (Belgium). FB (n = 11; 24–31 wk gestation) samples from interruption of pregnancy were obtained with approval of the Erasme Hospital (Université Libre de Bruxelles) Ethics Committee, and umbilical CB (n = 16; >37 wk gestation) samples after delivery were obtained with approval of the University Hospital Center Saint-Pierre (Belgium). For all the samples used in this work, written informed consent was given.

Isolation of cells

Cell suspension from FT and PNT samples was obtained as previously described (McGovern et al., 2017; Van Coppernolle et al., 2009). γδ T cells from postnatal suspensions were isolated by positive selection using anti-TCRγδ magnetic activated cell sorting beads (Miltenyi Biotec) according to the manufacturer's instruction. Note that since it appears that the phosphoantigen-reactive Vγ9Vδ2 subset follows different rules compared with all the other human γδ T cell subsets regarding the CDR3 repertoire, we excluded the Vγ9Vδ2 subset. Indeed, in contrast to other subsets (such as $Vδ1^+$ and $Vγ9^-Vδ2^+$), Vγ9Vδ2 T cells express a semi-invariant TCR in AB and CB (Davey et al., 2017, 2018; Dimova et al., 2015; Papadopoulou et al., 2019; Ravens et al., 2017; Sherwood et al., 2011). Thus, the $γδ^+$ fraction was further sorted into $CD3^+TCRγδ^+$ without the $Vγ9^+Vδ2^+$ subset (nonVγ9Vδ2 γδ T cells), while from the γδ-negative fraction, αβ T cells ($CD3^+$ $TCRγδ^-$) were sorted (all around 10,000 cells, except when indicated) on a FACS Aria III cell sorter (BD Biosciences), snap-frozen in liquid nitrogen, and stored at −80°C for later RNA extraction. The mean purity was 95.0% (percentage of living cells).

Mononuclear cells were collected from blood samples (FB, CB, and AB) by Lymphoprep gradient centrifugation (Axis-Shield). Cell suspensions from FL samples were obtained as previously described (McGovern et al., 2017). $CD34^+$ HSPCs were isolated by anti-CD34 magnetic activated cell sorting beads (Miltenyi Biotec) by positive selection according to the manufacturer's instruction. Purity was 92.0%, and the percentage of $CD3^+TCRγδ^+$ cells was <0.6 (percentage of living cells).

OP9DL1 co-cultures

OP9DL1 cells were obtained from Dr. J.C. Zuniga Pflucker (University of Toronto, Toronto, Canada; La Motte-Mohs et al., 2005). Isolated $CD34^+$ cells were seeded in a 6-well culture plate

(5×10^5 cells/well) containing a monolayer of OP9DL1 cells in MEMα (Gibco BRL Life Technologies) supplemented with 20% FBS (Sigma-Aldrich), 1% nonessential amino acids, 1% glutamine, and 1% penicillin/streptomycin (Pen/Strep; Lonza) in the presence of 10 ng/ml IL-7 (R&D Systems), 10 ng/ml Flt3L (PeproTech), and 5 ng/ml stem cell factor (SCF; PeproTech). Every 4–5 d cells were harvested by vigorous pipetting and transferred in a new 6-well plate (5×10^5–5×10^6 cells/well; Van Coppernolle et al., 2009). Differentiation of HSPCs was analyzed by flow cytometry, characterized by the gradual loss of the HSPC marker CD34 and parallel increase of the T progenitor marker CD7 (Van Coppernolle et al., 2009; La Motte-Mohs et al., 2005). After 2 or 4 wk in co-culture, >96% of living cells were $CD7^+$. The CD1a marker was used to assess the maturation state. After ∼30 d in co-culture with OP9DL1 cells (Fig. 4 A), HPSC-derived cells were stained, and $CD3^+TCR\gamma\delta^+$ (defined as γδ T cells) and $CD3^-TCR\gamma\delta^-$ (defined as progenitors) cell populations were sorted (2,000–30,000 γδ cells, 100,000–150,000 precursor cells) on a FACS Aria III cell sorter, snap-frozen in liquid nitrogen, and stored at −80°C for later RNA extraction. Purity was >98% (percentage of living cells).

Retroviral vectors, transfection, and transduction

Human *LIN28B* (NM_001004317) was amplified via PCR from MSCV-Lin28b-PIG (gift from the laboratory of Joshua Mendell, University of Texas Southwestern Medical Center, Dallas, TX) introducing BamHI restriction enzyme sites (Helsmoortel et al., 2016). The amplified PCR product was cloned into the BamHI site of the retroviral LZRS-ires-eGFP plasmid, and retroviral particles were produced as previously described (Van Coppernolle et al., 2012). We used CB $CD34^+$ cells, rather than AB $CD34^+$ cells, in order to transduce with the retroviral vectors because of their availability and the efficiency of $CD7^+$ progenitor generation from $CD34^+$ cells in the OP9DL1 cultures. CB $CD34^+$ cells were preactivated for 48 h in Iscove's Modified Dulbecco's Media (Lonza) supplemented with 10% FBS, 1% nonessential amino acids, 1% glutamine, and 1% Pen/Strep in the presence of 50 ng/ml SCF, 50 ng/ml Flt3L, and 20 ng/ml thrombopoietin (PeproTech). Cells were then transferred on a nontissue culture plate coated with retronectin (TaKaRa) in the presence of supernatant containing the *LIN28B*-expressing or control viral construct, Flt3-liter (0.2 µg/ml), SCF (0.2 µg/ml), and thrombopoietin (40 ng/ml), followed by a centrifugation step for 90 min at 710 *g* at 32°C. After 2 d in culture at 37°C, cells were washed with PBS and seeded in a 6-well culture plate containing OP9DL1 cells as described above. The transduction efficiency was assessed as the percentage of GFP-positive cells by flow cytometry (mean transduction efficiency was 51% for Lin28b and 59% for control).

Flow cytometry and time-of-flight mass cytometry (CyToF)

The following antibodies were used for flow cytometry: CD3-Pacific Blue (clones SP34-2, UCHT1; BD Biosciences), CD3-V500 (UCHT1; BD Biosciences), CD3-V510 (UCHT1; BD Biosciences), CD3-ECD (UCHT1; Beckman Coulter), TCRγδ-FITC (11F2; BD Biosciences), TCRγδ-PE (11F2; BD Biosciences), TCRγδ-APC (11F2; Miltenyi Biotec), Vδ1-FITC (TS-1; Thermo Scientific), Vδ1-PE (REA173; Miltenyi Biotec), Vδ2-FITC (IMMU 389; Beckman Coulter), Vδ2-Pacific Blue (IMMU 389; Beckman Coulter), Vδ9-PC5 (IMMU 360; Beckman Coulter), CD7-PE-Cy7 (M-T701; BD Biosciences), CD7-V450 (M-T701; BD Biosciences), CD34-PE (AC136; Miltenyi Biotec), CD1a-eFluor450 (HI149; eBioscience), CD1a-PE-Cy7 (HI149; eBioscience), CD1a-PE/Dazzle594 (HI149; BioLegend), CD4-V500 (RPA-T4; BD Biosciences), CD27-PE-Cy7 (M-T271; BD Biosciences), CD27-PE (M-T271; BD Biosciences), Granzyme A-Pacific Blue (CB9; BioLegend), IFNγ-V450 (B27; BD Biosciences), and Tbet-PE (eBio4B10; eBioscience). To assess cell viability, cells were stained with the fixable viability dye Zombie NIR or Zombie red (BioLegend). Cells were washed with PBS (Lonza) supplemented with 0.1% BSA (Sigma-Aldrich) followed by incubation in PBS + 0.1% BSA at 4°C in the dark for 20 min. Cells were then washed again with PBS + 0.1% BSA before fixation in 1% paraformaldehyde (Sigma-Aldrich). Intracellular staining for granzyme A was performed with a Cytofix/Cytoperm kit (BD Biosciences) while the simultaneous detection of IFNγ and Tbet was performed with the Foxp3/transcription factor staining buffer set (eBioscience). For the detection of IFNγ and Tbet, thymocytes were cultured for 4 h in the presence or absence of 10 ng/ml PMA (Sigma-Aldrich) and 2 µM ionomycin calcium salt (Sigma-Aldrich). 5 µg/ml brefeldin A (Sigma-Aldrich) and 2 µM monensin (Sigma-Aldrich) were added 30 min after the beginning of the culture. Cells were run on the CyAn Cyan ADP cytometer (Dako Cytomation) or on the BD LSRFortessa cell analyzer, and data were analyzed using FlowJo software (v9.8.5). Fetal thymocytes were stained as previously described and then analyzed using CyToF (Chew et al., 2019); here, we gated on fetal γδ and αβ thymocytes in order to analyze the expression of IFNγ and Tbet with FlowJo.

TRG, TRD, TRA, and TRB repertoire analysis

RNA derived from sorted cell populations and from cells harvested from total OP9DL1 co-cultures was isolated following the RNAeasy micro (for sorted cells and cells from total OP9DL1 co-culture when the number of cells was $<10^6$) and mini (cells from total OP9-DL1 culture when the number of cells was $>10^6$) kit protocol (Qiagen). cDNA was generated performing a template-switch anchored RT-PCR. RNA was reverse transcribed via a template-switch cDNA reaction using TRGC (5′-CAAGAAGAC AAAGGTATGTTCCAG-3′)- and TRDC (5′-GTAGAATTCCTTCAC CAGACAAG-3′)-specific primers in the same reaction tube, a template-switch adaptor (5′-AAGCAGTGGTATCAACGCAGAGT ACATrGrGrG-3′), and the Superscript II RT enzyme (Invitrogen). The TRGC primer binds both TRGC1 and TRGC2. The cDNA was then purified using AMPure XP Beads (Agencourt). Amplification of the TRG and TRD region was achieved using a specific TRGC primer (binding also both TRGC1 and TRGC2 5′-*GTCTCGTGGGCTCGGAGATGTGTATAAGAGACAG*AATAGTGGGCTT GGGGGAAACATCTGCAT-3′, adapter in italic), a specific TRDC primer (5′-*GTCTCGTGGGCTCGGAGATGTGTATAAGAGACAG*ACG GATGGTTTGGTATGAGGCTGACTTCT-3′, adapter in italic) and a primer complementary to the template-switch adapter (5′-*TCG TCGGCAGCGTCAGATGTGTATAAGAGACAG*AAGCAGTGGTATCAA CGCAG-3′, adapter in italic) with the KAPA Real-Time Library Amplification Kit (Kapa Biosystems). Adapters were required

for subsequent sequencing reactions. After purification with AMPure XP Beads, an index PCR with Illumina sequencing adapters was performed using the Nextera XT Index Kit. This second PCR product was again purified with AMPure XP beads. HTS of the generated amplicon products containing the CDR3γ or CDR3δ sequences was performed on an Illumina MiSeq platform using the V2 300 kit, with 151 bp at the 3′ end (read 2) and 151 bp at the 5′ end (read 1; at the GIGA Center, University of Liège, Belgium). HTS analysis of TRA and TRB loci was performed as previously described (Van Caeneghem et al., 2017).

CDR3 sequences were obtained by aligning raw sequencing reads from fastq files (read 1 plus read 2) to reference V, D, and J genes from the GenBank database for TRG or TRD loci using the MiXCR software version 2.1.11 (Bolotin et al., 2015). Default parameters were used except to assemble TRDD and TRBD gene segments where three instead of five consecutive nucleotides were applied as the assemble parameter. CDR3 sequences were then exported and analyzed using VDJtools software version 1.1.9 using default settings (Shugay et al., 2015). Sequences out of frame and containing stop codons were excluded from the analysis. Overlap analysis was performed as the geometric mean of relative overlap frequencies between repertoires (F metrics of VDJtools software). Tree maps were created using the Treemap Package.

Gene expression profile analysis

RNA derived from sorted cell populations was isolated following the RNAeasy micro kit protocol (Qiagen). RNA quality was checked using a Bioanalyzer 2100 (Agilent Technologies). Indexed cDNA libraries were obtained using the Ovation Solo RNA-Seq System (NuGen) following the manufacturer's recommendation. The multiplexed libraries were loaded on a NovaSeq 6000 (Illumina) using an S2 flow cell, and sequences were produced using a 200 Cycle Kit. Paired-end reads were mapped against the human reference genome GRCh38 using STAR software to generate read alignments for each sample. Annotations Homo_sapiens.GRCh38.90.gtf were obtained from ftp.Ensembl.org. After transcript assembling, gene level counts were obtained using HTSeq. Differential expression (FT versus PNT γδ thymoctyes, FT versus PNT AB thymocytes, and FL-derived versus AB-derived γδ T cells) was analyzed using EdgeR quasi-likelihood (Robinson et al., 2010) running under the Degust platform, where also the Volcano plots (logFoldChange(FC) versus logFalseDiscoveryRate(FDR)) were generated (http://degust.erc.monash.edu/). Only genes with a minimum count per million of 1 in each replicate were included. Functional annotation was verified using the functional annotation tool DAVID (Huang et al., 2009). Gene sets of FT versus γδ thymocytes and FL-derived versus AB-derived γδ T cells (logFC >0.7, FDR <0.1) were generated for GSEA analysis (Table S1). For the Lin28b versus control comparison, a paired analysis with EdgeR was performed (Robinson et al., 2010). Heatmaps were generated using the Mev software: data were log2-transformed and median centered by gene (Howe et al., 2011). GSEA analysis was performed with the default value of 1,000 permutations (permutation type gene set; Subramanian et al., 2005). Datasets were compared in an unbiased way with GSEA using the gene sets derived from the C7 immunological gene signature from the MSigDB containing 4,872 immunological gene sets (Godec et al., 2016); the following gene sets from this analysis were included: activated human T cells, GSE28726_NAIVE_VS_ACTIVATED_CD4_TCELL_DN; activated mouse T cells, GSE10239_NAIVE_VS_DAY4.5_EFF_CD8_TCELL_DN; IL15-stimulated human NK cells, GSE22886_UNSTIM_VS_IL15_STIM_NKCELL_DN; IL15-stimulated mouse NK cells, GSE7764_IL15_TREATED_VS_CTRL_NK_CELL_24H_UP. The RNA sequencing (RNAseq) data are deposited at the GEO repository, under accession no. GSE128163.

Statistical analysis

All statistical analyses were performed using GraphPad Prism 5. Two-tailed Student's *t* test and paired *t* test were used for normally distributed data; Mann Whitney *U* and Wilcoxon matched paired tests were used for nonparametric data. Differences between more than two groups were analyzed using Kruskal–Wallis ANOVA and Dunn's post-tests for nonparametric data. *, $P < 0.05$; **, $P < 0.01$; ***, $P < 0.001$.

Online supplemental material

Fig. S1 shows flow cytometry data on FTs and PNTs. Fig. S2 shows TCR/CDR3 data of FT and PNT γδ thymocytes. Fig. S3 shows CDR3 data on αβ thymocytes. Fig. S4 shows that TRDV10 RNA contains the leader intron introducing a stop codon. Fig. S5 shows TCR/CDR3 and RNAseq data of Lin28b- versus control-transduced CB HSPC-derived γδ T cells. Table S1 shows a list of differentially expressed genes between FT and PNT γδ thymocytes and between FL and AB γδ T cells.

Acknowledgments

We are grateful to the mothers who participated in this study and the midwives of the Hôpital Erasme (Université Libre de Bruxelles) and Centre Hospitalier Universitaire Saint-Pierre delivery room who helped with the recruitment of the mothers. We thank Adrian Hayday and Pierre Vantourout (King's College London and Francis Crick Institute, London, UK) for insightful discussions. We thank the GIGA Genomics platform (Latifa Karim and Wouter Coppieters) and the Brussels Interuniversity Genomics High Throughput core platform (Anne Lefort and Frédérick Libert) for their outstanding technical support.

This work was supported by the Fonds De La Recherche Scientifique (Télévie 7.4555.14 and J.0078.13), the Fonds Gaston Ithier and the European Commission (Marie Skłodowska-Curie Actions [MSCA] project 751954). P. Tieppo is supported by the Fonds De La Recherche Scientifique (Télévie) and the Fondation Rose et Jean Hoguet; M. Papadopoulou is supported by the Fonds De La Recherche Scientifique (FRIA); L. Ma is supported by the Chinese Scholarship Council; N. McGovern is supported by the Wellcome Trust; and N. Dauby is a post-doctoral research fellow of the Fonds De La Recherche Scientifique. This article is published with the support of the Fondation Universitaire of Belgium.

The authors declare no competing financial interests.

Author contributions: P. Tieppo, M. Papadopoulou, D. Gatti, N. McGovern, and L. Ma designed and undertook experiments. J.K.Y. Chan, F. Gosselin, G. Goetgeluk, K. Weening, N. Dauby, A. Cogan, C. Donner, and F. Ginhoux designed, prepared, and provided critical human cell material and reagents. P. Tieppo, M. Papadopoulou, B. Vandekerckhove, and D. Vermijlen processed and interpreted data. P. Tieppo, M. Papadopoulou, and N. Dauby revised the manuscript. B. Vandekerckhove and D. Vermijlen wrote the manuscript. D. Vermijlen designed the study.

Submitted: 31 March 2019
Revised: 13 September 2019
Accepted: 29 October 2019

References

Asarnow, D.M., D. Cado, and D.H. Raulet. 1993. Selection is not required to produce invariant T-cell receptor γ-gene junctional sequences. *Nature.* 362:158–160. https://doi.org/10.1038/362158a0

Beaudin, A.E., S.W. Boyer, J. Perez-Cunningham, G.E. Hernandez, S.C. Derderian, C. Jujjavarapu, E. Aaserude, T. MacKenzie, and E.C. Forsberg. 2016. A transient developmental hematopoietic stem cell gives rise to innate-like B and T cells. *Cell Stem Cell.* 19:768–783. https://doi.org/10.1016/j.stem.2016.08.013

Bolotin, D.A., S. Poslavsky, I. Mitrophanov, M. Shugay, I.Z. Mamedov, E.V. Putintseva, and D.M. Chudakov. 2015. MiXCR: software for comprehensive adaptive immunity profiling. *Nat. Methods.* 12:380–381. https://doi.org/10.1038/nmeth.3364

Boyden, L.M., J.M. Lewis, S.D. Barbee, A. Bas, M. Girardi, A.C. Hayday, R.E. Tigelaar, and R.P. Lifton. 2008. Skint1, the prototype of a newly identified immunoglobulin superfamily gene cluster, positively selects epidermal gammadelta T cells. *Nat. Genet.* 40:656–662. https://doi.org/10.1038/ng.108

Boyerinas, B., S.-M. Park, N. Shomron, M.M. Hedegaard, J. Vinther, J.S. Andersen, C. Feig, J. Xu, C.B. Burge, and M.E. Peter. 2008. Identification of let-7-regulated oncofetal genes. *Cancer Res.* 68:2587–2591. https://doi.org/10.1158/0008-5472.CAN-08-0264

Bronevetsky, Y., T.D. Burt, and J.M. McCune. 2016. Lin28b regulates fetal regulatory T cell differentiation through modulation of TGF-β signaling. *J. Immunol.* 197:4344–4350. https://doi.org/10.4049/jimmunol.1601070

Chen, X., L. Poncette, and T. Blankenstein. 2017. Human TCR-MHC coevolution after divergence from mice includes increased nontemplate-encoded CDR3 diversity. *J. Exp. Med.* 214:3417–3433. https://doi.org/10.1084/jem.20161784

Chew, V., Y.H. Lee, L. Pan, N.J.M. Nasir, C.J. Lim, C. Chua, L. Lai, S.N. Hazirah, T.K.H. Lim, B.K.P. Goh, et al. 2019. Immune activation underlies a sustained clinical response to Yttrium-90 radioembolisation in hepatocellular carcinoma. *Gut.* 68:335–346. https://doi.org/10.1136/gutjnl-2017-315485

Chien, Y.H., and Y. Konigshofer. 2007. Antigen recognition by gammadelta T cells. *Immunol. Rev.* 215:46–58. https://doi.org/10.1111/j.1600-065X.2006.00470.x

Chien, Y.H., C. Meyer, and M. Bonneville. 2014. γδ T cells: first line of defense and beyond. *Annu. Rev. Immunol.* 32:121–155. https://doi.org/10.1146/annurev-immunol-032713-120216

Davey, M.S., C.R. Willcox, S.P. Joyce, K. Ladell, S.A. Kasatskaya, J.E. McLaren, S. Hunter, M. Salim, F. Mohammed, D.A. Price, et al. 2017. Clonal selection in the human Vδ1 T cell repertoire indicates γδ TCR-dependent adaptive immune surveillance. *Nat. Commun.* 8:14760. https://doi.org/10.1038/ncomms14760

Davey, M.S., C.R. Willcox, S. Hunter, S.A. Kasatskaya, E.B.M. Remmerswaal, M. Salim, F. Mohammed, F.J. Bemelman, D.M. Chudakov, Y.H. Oo, and B.E. Willcox. 2018. The human Vδ2$^+$ T-cell compartment comprises distinct innate-like Vγ9$^+$ and adaptive Vγ9$^-$ subsets. *Nat. Commun.* 9:1760. https://doi.org/10.1038/s41467-018-04076-0

De Creus, A., K. Van Beneden, F. Stevenaert, V. Debacker, J. Plum, and G. Leclercq. 2002. Developmental and functional defects of thymic and epidermal V γ 3 cells in IL-15-deficient and IFN regulatory factor-1-deficient mice. *J. Immunol.* 168:6486–6493. https://doi.org/10.4049/jimmunol.168.12.6486

de Vasconcellos, J.F., L. Tumburu, C. Byrnes, Y.T. Lee, P.C. Xu, M. Li, A. Rabel, B.A. Clarke, N.R. Guydosh, R.L. Proia, and J.L. Miller. 2017. IGF2BP1 overexpression causes fetal-like hemoglobin expression patterns in cultured human adult erythroblasts. *Proc. Natl. Acad. Sci. USA.* 114:E5664–E5672. https://doi.org/10.1073/pnas.1609552114

Di Lorenzo, B., J. Déchanet-Merville, and B. Silva-Santos. 2017. Peripheral clonal selection shapes the human γδ T-cell repertoire. *Cell. Mol. Immunol.* 14:733–735. https://doi.org/10.1038/cmi.2017.51

Di Lorenzo, B., S. Ravens, and B. Silva-Santos. 2019. High-throughput analysis of the human thymic Vδ1$^+$ T cell receptor repertoire. *Sci. Data.* 6:115. https://doi.org/10.1038/s41597-019-0118-2

Di Marco Barros, R., N.A. Roberts, R.J. Dart, P. Vantourout, A. Jandke, O. Nussbaumer, L. Deban, S. Cipolat, R. Hart, M.L. Iannitto, et al. 2016. Epithelia use butyrophilin-like molecules to shape organ-specific. *Cell.* 167:203–218.e17. https://doi.org/10.1016/j.cell.2016.08.030

Dimova, T., M. Brouwer, F. Gosselin, J. Tassignon, O. Leo, C. Donner, A. Marchant, and D. Vermijlen. 2015. Effector Vγ9Vδ2 T cells dominate the human fetal γδ T-cell repertoire. *Proc. Natl. Acad. Sci. USA.* 112:E556–E565. https://doi.org/10.1073/pnas.1412058112

Do, J.S., P.J. Fink, L. Li, R. Spolski, J. Robinson, W.J. Leonard, J.J. Letterio, and B. Min. 2010. Cutting edge: spontaneous development of IL-17-producing γ δ T cells in the thymus occurs via a TGF-β 1-dependent mechanism. *J. Immunol.* 184:1675–1679. https://doi.org/10.4049/jimmunol.0903539

Dokouhaki, P., N.W. Schuh, B. Joe, C.A.D. Allen, S.D. Der, M.-S. Tsao, and L. Zhang. 2013. NKG2D regulates production of soluble TRAIL by ex vivo expanded human γδ T cells. *Eur. J. Immunol.* 43:3175–3182. https://doi.org/10.1002/eji.201243150

Gentek, R., C. Ghigo, G. Hoeffel, A. Jorquera, R. Msallam, S. Wienert, F. Klauschen, F. Ginhoux, and M. Bajénoff. 2018. Epidermal γδ T cells originate from yolk sac hematopoiesis and clonally self-renew in the adult. *J. Exp. Med.* 215:2994–3005. https://doi.org/10.1084/jem.20181206

Ginhoux, F., and S. Jung. 2014. Monocytes and macrophages: developmental pathways and tissue homeostasis. *Nat. Rev. Immunol.* 14:392–404. https://doi.org/10.1038/nri3671

Godec, J., Y. Tan, A. Liberzon, P. Tamayo, S. Bhattacharya, A.J. Butte, J.P. Mesirov, and W.N. Haining. 2016. Compendium of immune signatures identifies conserved and species-specific biology in response to inflammation. *Immunity.* 44:194–206. https://doi.org/10.1016/j.immuni.2015.12.006

Guo, X.J., P. Dash, J.C. Crawford, E.K. Allen, A.E. Zamora, D.F. Boyd, S. Duan, R. Bajracharya, W.A. Awad, N. Apiwattanakul, et al. 2018. Lung. *Immunity.* 49:531–544.e6. https://doi.org/10.1016/j.immuni.2018.07.011

Haas, J.D., F.H. González, S. Schmitz, V. Chennupati, L. Föhse, E. Kremmer, R. Förster, and I. Prinz. 2009. CCR6 and NK1.1 distinguish between IL-17A and IFN-γ-producing gammadelta effector T cells. *Eur. J. Immunol.* 39:3488–3497. https://doi.org/10.1002/eji.200939922

Haas, J.D., S. Ravens, S. Düber, I. Sandrock, L. Oberdörfer, E. Kashani, V. Chennupati, L. Föhse, R. Naumann, S. Weiss, et al. 2012. Development of interleukin-17-producing γδ T cells is restricted to a functional embryonic wave. *Immunity.* 37:48–59. https://doi.org/10.1016/j.immuni.2012.06.003

Havran, W.L., and J.P. Allison. 1990. Origin of Thy-1$^+$ dendritic epidermal cells of adult mice from fetal thymic precursors. *Nature.* 344:68–70. https://doi.org/10.1038/344068a0

Hayday, A.C. 2000. [γ][δ] cells: a right time and a right place for a conserved third way of protection. *Annu. Rev. Immunol.* 18:975–1026. https://doi.org/10.1146/annurev.immunol.18.1.975

Hayday, A.C. 2019. T cell update: adaptate orchestrators of immune surveillance. *J. Immunol.* 203:311–320. https://doi.org/10.4049/jimmunol.1800934

Helsmoortel, H.H., B. De Moerloose, T. Pieters, F. Ghazavi, S. Bresolin, H. Cavé, A. de Vries, V. de Haas, C. Flotho, V. Labarque, et al. 2016. LIN28B is over-expressed in specific subtypes of pediatric leukemia and regulates lncRNA H19. *Haematologica.* 101:e240–e244. https://doi.org/10.3324/haematol.2016.143818

Howe, E.A., R. Sinha, D. Schlauch, and J. Quackenbush. 2011. RNA-Seq analysis in MeV. *Bioinformatics.* 27:3209–3210. https://doi.org/10.1093/bioinformatics/btr490

Huang, W., B.T. Sherman, and R.A. Lempicki. 2009. Systematic and integrative analysis of large gene lists using DAVID bioinformatics resources. *Nat. Protoc.* 4:44–57. https://doi.org/10.1038/nprot.2008.211

Ikuta, K., T. Kina, I. MacNeil, N. Uchida, B. Peault, Y.H. Chien, and I.L. Weissman. 1990. A developmental switch in thymic lymphocyte

maturation potential occurs at the level of hematopoietic stem cells. *Cell.* 62:863–874. https://doi.org/10.1016/0092-8674(90)90262-D

Itohara, S., P. Mombaerts, J. Lafaille, J. Iacomini, A. Nelson, A.R. Clarke, M.L. Hooper, A. Farr, and S. Tonegawa. 1993. T cell receptor delta gene mutant mice: independent generation of alpha beta T cells and programmed rearrangements of gamma delta TCR genes. *Cell.* 72:337–348. https://doi.org/10.1016/0092-8674(93)90112-4

Jiang, S., and D. Baltimore. 2016. RNA-binding protein Lin28 in cancer and immunity. *Cancer Lett.* 375:108–113. https://doi.org/10.1016/j.canlet.2016.02.050

Kallemeijn, M.J., F.G. Kavelaars, M.Y. van der Klift, I.L.M. Wolvers-Tettero, P.J.M. Valk, J.J.M. van Dongen, and A.W. Langerak. 2018. Next-generation sequencing analysis of the human TCR. *Front. Immunol.* 9: 448. https://doi.org/10.3389/fimmu.2018.00448

Kan, B., H.R. Razzaghian, and P.M. Lavoie. 2016. An immunological perspective on neonatal sepsis. *Trends Mol. Med.* 22:290–302. https://doi.org/10.1016/j.molmed.2016.02.001

Kazen, A.R., and E.J. Adams. 2011. Evolution of the V, D, and J gene segments used in the primate gammadelta T-cell receptor reveals a dichotomy of conservation and diversity. *Proc. Natl. Acad. Sci. USA.* 108:E332–E340. https://doi.org/10.1073/pnas.1105105108

Kohlgruber, A.C., S.T. Gal-Oz, N.M. LaMarche, M. Shimazaki, D. Duquette, H.-F. Koay, H.N. Nguyen, A.I. Mina, T. Paras, A. Tavakkoli, et al. 2018. γδ T cells producing interleukin-17A regulate adipose regulatory T cell homeostasis and thermogenesis. *Nat. Immunol.* 19:464–474. https://doi.org/10.1038/s41590-018-0094-2

Kollmann, T.R., B. Kampmann, S.K. Mazmanian, A. Marchant, and O. Levy. 2017. Protecting the newborn and young infant from infectious diseases: lessons from immune ontogeny. *Immunity.* 46:350–363. https://doi.org/10.1016/j.immuni.2017.03.009

Kovalovsky, D., O.U. Uche, S. Eladad, R.M. Hobbs, W. Yi, E. Alonzo, K. Chua, M. Eidson, H.-J. Kim, J.S. Im, et al. 2008. The BTB-zinc finger transcriptional regulator PLZF controls the development of invariant natural killer T cell effector functions. *Nat. Immunol.* 9:1055–1064. https://doi.org/10.1038/ni.1641

Krangel, M.S., H. Yssel, C. Brocklehurst, and H. Spits. 1990. A distinct wave of human T cell receptor γ/δ lymphocytes in the early fetal thymus: evidence for controlled gene rearrangement and cytokine production. *J. Exp. Med.* 172:847–859. https://doi.org/10.1084/jem.172.3.847

Kreslavsky, T., A.K. Savage, R. Hobbs, F. Gounari, R. Bronson, P. Pereira, P.P. Pandolfi, A. Bendelac, and H. von Boehmer. 2009. TCR-inducible PLZF transcription factor required for innate phenotype of a subset of gammadelta T cells with restricted TCR diversity. *Proc. Natl. Acad. Sci. USA.* 106:12453–12458. https://doi.org/10.1073/pnas.0903895106

Kreslavsky, T., J.B. Wong, M. Fischer, J.A. Skok, and M. Busslinger. 2018. Control of B-1a cell development by instructive BCR signaling. *Curr. Opin. Immunol.* 51:24–31. https://doi.org/10.1016/j.coi.2018.01.001

Krishnan, S., I.E. Prise, K. Wemyss, L.P. Schenck, H.M. Bridgeman, F.A. McClure, T. Zangerle-Murray, C. O'Boyle, T.A. Barbera, F. Mahmood, et al. 2018. Amphiregulin-producing γδ T cells are vital for safeguarding oral barrier immune homeostasis. *Proc. Natl. Acad. Sci. USA.* 115: 10738–10743. https://doi.org/10.1073/pnas.1802320115

La Motte-Mohs, R.N., E. Herer, and J.C. Zúñiga-Pflücker. 2005. Induction of T-cell development from human cord blood hematopoietic stem cells by Delta-like 1 in vitro. *Blood.* 105:1431–1439. https://doi.org/10.1182/blood-2004-04-1293

Laird, R.M., K. Laky, and S.M. Hayes. 2010. Unexpected role for the B cell-specific Src family kinase B lymphoid kinase in the development of IL-17-producing γδ T cells. *J. Immunol.* 185:6518–6527. https://doi.org/10.4049/jimmunol.1002766

Lewis, D.B., and C.B. Wilson. 2006. Developmental immunology and role of host defenses in fetal and neonatal susceptibility to infection. *In* Infectious Disease of the Fetus and Newborn Infant. J.S. Remington and J.O. Klein, editors. Elsevier Saunders, Philadelphia, PA. 87–210. https://doi.org/10.1016/B0-72-160537-0/50006-2

Mamedov, M.R., A. Scholzen, R.V. Nair, K. Cumnock, J.A. Kenkel, J.H.M. Oliveira, D.L. Trujillo, N. Saligrama, Y. Zhang, F. Rubelt, et al. 2018. A macrophage colony-stimulating-factor-producing. *Immunity.* 48: 350–363.e7. https://doi.org/10.1016/j.immuni.2018.01.009

McGovern, N., A. Shin, G. Low, D. Low, K. Duan, L.J. Yao, R. Msallam, I. Low, N.B. Shadan, H.R. Sumatoh, et al. 2017. Human fetal dendritic cells promote prenatal T-cell immune suppression through arginase-2. *Nature.* 546:662–666. https://doi.org/10.1038/nature22795

McVay, L.D., S.R. Carding, K. Bottomly, and A.C. Hayday. 1991. Regulated expression and structure of T cell receptor gamma/delta transcripts in human thymic ontogeny. *EMBO J.* 10:83–91. https://doi.org/10.1002/j.1460-2075.1991.tb07923.x

Mestas, J., and C.C.W. Hughes. 2004. Of mice and not men: differences between mouse and human immunology. *J. Immunol.* 172:2731–2738. https://doi.org/10.4049/jimmunol.172.5.2731

Mold, J.E., J. Michaëlsson, T.D. Burt, M.O. Muench, K.P. Beckerman, M.P. Busch, T.H. Lee, D.F. Nixon, and J.M. McCune. 2008. Maternal alloantigens promote the development of tolerogenic fetal regulatory T cells in utero. *Science.* 322:1562–1565. https://doi.org/10.1126/science.1164511

Mold, J.E., S. Venkatasubrahmanyam, T.D. Burt, J. Michaëlsson, J.M. Rivera, S.A. Galkina, K. Weinberg, C.A. Stoddart, and J.M. McCune. 2010. Fetal and adult hematopoietic stem cells give rise to distinct T cell lineages in humans. *Science.* 330:1695–1699. https://doi.org/10.1126/science.1196509

Morita, C.T., C.M. Parker, M.B. Brenner, and H. Band. 1994. TCR usage and functional capabilities of human γ δ T cells at birth. *J. Immunol.* 153: 3979–3988.

Moss, E.G., R.C. Lee, and V. Ambros. 1997. The cold shock domain protein LIN-28 controls developmental timing in *C. elegans* and is regulated by the lin-4 RNA. *Cell.* 88:637–646. https://doi.org/10.1016/S0092-8674(00)81906-6

Muñoz-Ruiz, M., J.C. Ribot, A.R. Grosso, N. Gonçalves-Sousa, A. Pamplona, D.J. Pennington, J.R. Regueiro, E. Fernández-Malavé, and B. Silva-Santos. 2016. TCR signal strength controls thymic differentiation of discrete proinflammatory γδ T cell subsets. *Nat. Immunol.* 17:721–727. https://doi.org/10.1038/ni.3424

Pang, D.J., J.F. Neves, N. Sumaria, and D.J. Pennington. 2012. Understanding the complexity of γδ T-cell subsets in mouse and human. *Immunology.* 136:283–290. https://doi.org/10.1111/j.1365-2567.2012.03582.x

Papadopoulou, M., P. Tieppo, N. McGovern, F. Gosselin, J.K.Y. Chan, G. Goetgeluk, N. Dauby, A. Cogan, C. Donner, F. Ginhoux, et al. 2019. TCR sequencing reveals the distinct development of fetal and adult human Vγ9Vδ2 T Cells. *J. Immunol.* 203:1468–1479. https://doi.org/10.4049/jimmunol.1900592

Pobezinsky, L.A., R. Etzensperger, S. Jeurling, A. Alag, T. Kadakia, T.M. McCaughtry, M.Y. Kimura, S.O. Sharrow, T.I. Guinter, L. Feigenbaum, and A. Singer. 2015. Let-7 microRNAs target the lineage-specific transcription factor PLZF to regulate terminal NKT cell differentiation and effector function. *Nat. Immunol.* 16:517–524. https://doi.org/10.1038/ni.3146

Ramond, C., C. Berthault, O. Burlen-Defranoux, A.P. de Sousa, D. Guy-Grand, P. Vieira, P. Pereira, and A. Cumano. 2014. Two waves of distinct hematopoietic progenitor cells colonize the fetal thymus. *Nat. Immunol.* 15: 27–35. https://doi.org/10.1038/ni.2782

Ravens, S., C. Schultze-Florey, S. Raha, I. Sandrock, M. Drenker, L. Oberdörfer, A. Reinhardt, I. Ravens, M. Beck, R. Geffers, et al. 2017. Human γδ T cells are quickly reconstituted after stem-cell transplantation and show adaptive clonal expansion in response to viral infection. *Nat. Immunol.* 18:393–401. https://doi.org/10.1038/ni.3686

Ribeiro, M., H.C. Brigas, M. Temido-Ferreira, P.A. Pousinha, T. Regen, C. Santa, J.E. Coelho, I. Marques-Morgado, C.A. Valente, S. Omenetti, et al. 2019. Meningeal γδ T cell-derived IL-17 controls synaptic plasticity and short-term memory. *Sci. Immunol.* 4:eaay5199. https://doi.org/10.1126/sciimmunol.aay5199

Ribot, J.C., A. deBarros, D.J. Pang, J.F. Neves, V. Peperzak, S.J. Roberts, M. Girardi, J. Borst, A.C. Hayday, D.J. Pennington, and B. Silva-Santos. 2009. CD27 is a thymic determinant of the balance between interferon-γ- and interleukin 17-producing gammadelta T cell subsets. *Nat. Immunol.* 10:427–436. https://doi.org/10.1038/ni.1717

Ribot, J.C., S.T. Ribeiro, D.V. Correia, A.E. Sousa, and B. Silva-Santos. 2014. Human γδ thymocytes are functionally immature and differentiate into cytotoxic type 1 effector T cells upon IL-2/IL-15 signaling. *J. Immunol.* 192:2237–2243. https://doi.org/10.4049/jimmunol.1303119

Roberts, N.A., A.J. White, W.E. Jenkinson, G. Turchinovich, K. Nakamura, D.R. Withers, F.M. McConnell, G.E. Desanti, C. Benezech, S.M. Parnell, et al. 2012. Rank signaling links the development of invariant γδ T cell progenitors and Aire(+) medullary epithelium. *Immunity.* 36:427–437. https://doi.org/10.1016/j.immuni.2012.01.016

Robinson, M.D., D.J. McCarthy, and G.K. Smyth. 2010. edgeR: a Bioconductor package for differential expression analysis of digital gene expression data. *Bioinformatics.* 26:139–140. https://doi.org/10.1093/bioinformatics/btp616

Rock, E.P., P.R. Sibbald, M.M. Davis, and Y.H. Chien. 1994. CDR3 length in antigen-specific immune receptors. *J. Exp. Med.* 179:323–328. https://doi.org/10.1084/jem.179.1.323

Rowe, R.G., L.D. Wang, S. Coma, A. Han, R. Mathieu, D.S. Pearson, S. Ross, P. Sousa, P.T. Nguyen, A. Rodriguez, et al. 2016. Developmental regulation of myeloerythroid progenitor function by the Lin28b-let-7-Hmga2 axis. *J. Exp. Med.* 213:1497–1512. https://doi.org/10.1084/jem.20151912

Savage, A.K., M.G. Constantinides, J. Han, D. Picard, E. Martin, B. Li, O. Lantz, and A. Bendelac. 2008. The transcription factor PLZF directs the effector program of the NKT cell lineage. *Immunity*. 29:391–403. https://doi.org/10.1016/j.immuni.2008.07.011

Scheper, W., S. van Dorp, S. Kersting, F. Pietersma, C. Lindemans, S. Hol, S. Heijhuurs, Z. Sebestyen, C. Gründer, V. Marcu-Malina, et al. 2013. γδT cells elicited by CMV reactivation after allo-SCT cross-recognize CMV and leukemia. *Leukemia*. 27:1328–1338. https://doi.org/10.1038/leu.2012.374

Sherwood, A.M., C. Desmarais, R.J. Livingston, J. Andriesen, M. Haussler, C.S. Carlson, and H. Robins. 2011. Deep sequencing of the human TCRγ and TCRβ repertoires suggests that TCRβ rearranges after αβ and γδ T cell commitment. *Sci. Transl. Med.* 3:90ra61. https://doi.org/10.1126/scitranslmed.3002536

Shugay, M., D.V. Bagaev, M.A. Turchaninova, D.A. Bolotin, O.V. Britanova, E.V. Putintseva, M.V. Pogorelyy, V.I. Nazarov, I.V. Zvyagin, V.I. Kirgizova, et al. 2015. VDJtools: unifying post-analysis of T cell receptor repertoires. *PLOS Comput. Biol.* 11:e1004503. https://doi.org/10.1371/journal.pcbi.1004503

Silva-Santos, B., and J. Strid. 2017. γδ T cells get adaptive. *Nat. Immunol.* 18:370–372. https://doi.org/10.1038/ni.3705

Silva-Santos, B., K. Serre, and H. Norell. 2015. γδ T cells in cancer. *Nat. Rev. Immunol.* 15:683–691. https://doi.org/10.1038/nri3904

Smith, N.L., R.K. Patel, A. Reynaldi, J.K. Grenier, J. Wang, N.B. Watson, K. Nzingha, K.J. Yee Mon, S.A. Peng, A. Grimson, et al. 2018. Developmental origin governs $CD8^+$ T cell fate decisions during infection. *Cell*. 174:117–130.e14. https://doi.org/10.1016/j.cell.2018.05.029

Subramanian, A., P. Tamayo, V.K. Mootha, S. Mukherjee, B.L. Ebert, M.A. Gillette, A. Paulovich, S.L. Pomeroy, T.R. Golub, E.S. Lander, and J.P. Mesirov. 2005. Gene set enrichment analysis: a knowledge-based approach for interpreting genome-wide expression profiles. *Proc. Natl. Acad. Sci. USA*. 102:15545–15550. https://doi.org/10.1073/pnas.0506580102

Van Caeneghem, Y., S. De Munter, P. Tieppo, G. Goetgeluk, K. Weening, G. Verstichel, S. Bonte, T. Taghon, G. Leclercq, T. Kerre, et al. 2017. Antigen receptor-redirected T cells derived from hematopoietic precursor cells lack expression of the endogenous TCR/CD3 receptor and exhibit specific antitumor capacities. *OncoImmunology*. 6:e1283460. https://doi.org/10.1080/2162402X.2017.1283460

Van Coppernolle, S., G. Verstichel, F. Timmermans, I. Velghe, D. Vermijlen, M. De Smedt, G. Leclercq, J. Plum, T. Taghon, B. Vandekerckhove, and T. Kerre. 2009. Functionally mature CD4 and CD8 TCRalphabeta cells are generated in OP9-DL1 cultures from human CD34+ hematopoietic cells. *J. Immunol.* 183:4859–4870. https://doi.org/10.4049/jimmunol.0900714

Van Coppernolle, S., S. Vanhee, G. Verstichel, S. Snauwaert, A. van der Spek, I. Velghe, M. Sinnesael, M.H. Heemskerk, T. Taghon, G. Leclercq, et al. 2012. Notch induces human T-cell receptor γδ+ thymocytes to differentiate along a parallel, highly proliferative and bipotent CD4 CD8 double-positive pathway. *Leukemia*. 26:127–138. https://doi.org/10.1038/leu.2011.324

van de Laar, L., W. Saelens, S. De Prijck, L. Martens, C.L. Scott, G. Van Isterdael, E. Hoffmann, R. Beyaert, Y. Saeys, B.N. Lambrecht, and M. Guilliams. 2016. Yolk sac macrophages, fetal liver, and adult monocytes can colonize an empty niche and develop into functional tissue-resident macrophages. *Immunity*. 44:755–768. https://doi.org/10.1016/j.immuni.2016.02.017

Van de Walle, I., G. De Smet, M. De Smedt, B. Vandekerckhove, G. Leclercq, J. Plum, and T. Taghon. 2009. An early decrease in Notch activation is required for human TCR-alphabeta lineage differentiation at the expense of TCR-gammadelta T cells. *Blood*. 113:2988–2998. https://doi.org/10.1182/blood-2008-06-164871

Vermijlen, D., and I. Prinz. 2014. Ontogeny of innate T lymphocytes—some innate lymphocytes are more innate than others. *Front. Immunol.* 5:486. https://doi.org/10.3389/fimmu.2014.00486

Vermijlen, D., M. Brouwer, C. Donner, C. Liesnard, M. Tackoen, M. Van Rysselberge, N. Twité, M. Goldman, A. Marchant, and F. Willems. 2010. Human cytomegalovirus elicits fetal gammadelta T cell responses in utero. *J. Exp. Med.* 207:807–821. https://doi.org/10.1084/jem.20090348

Wells, A.C., K.A. Daniels, C.C. Angelou, E. Fagerberg, A.S. Burnside, M. Markstein, D. Alfandari, R.M. Welsh, E.L. Pobezinskaya, and L.A. Pobezinsky. 2017. Modulation of let-7 miRNAs controls the differentiation of effector CD8 T cells. *eLife*. 6:e26398. https://doi.org/10.7554/eLife.26398

Yuan, J., C.K. Nguyen, X. Liu, C. Kanellopoulou, and S.A. Muljo. 2012. Lin28b reprograms adult bone marrow hematopoietic progenitors to mediate fetal-like lymphopoiesis. *Science*. 335:1195–1200. https://doi.org/10.1126/science.1216557

Zhang, X.M., C. Tonnelle, M.P. Lefranc, and S. Huck. 1994. T cell receptor γ cDNA in human fetal liver and thymus: variable regions of γ chains are restricted to V γ I or V9, due to the absence of splicing of the V10 and V11 leader intron. *Eur. J. Immunol.* 24:571–578. https://doi.org/10.1002/eji.1830240312

Zhang, Y., D. Cado, D.M. Asarnow, T. Komori, F.W. Alt, D.H. Raulet, and J.P. Allison. 1995. The role of short homology repeats and TdT in generation of the invariant γ δ antigen receptor repertoire in the fetal thymus. *Immunity*. 3:439–447. https://doi.org/10.1016/1074-7613(95)90173-6

Zuberbuehler, M.K., M.E. Parker, J.D. Wheaton, J.R. Espinosa, H.R. Salzler, E. Park, and M. Ciofani. 2019. The transcription factor c-Maf is essential for the commitment of IL-17-producing γδ T cells. *Nat. Immunol.* 20:73–85. https://doi.org/10.1038/s41590-018-0274-0

Supplemental material

Tieppo et al., https://doi.org/10.1084/jem.20190580

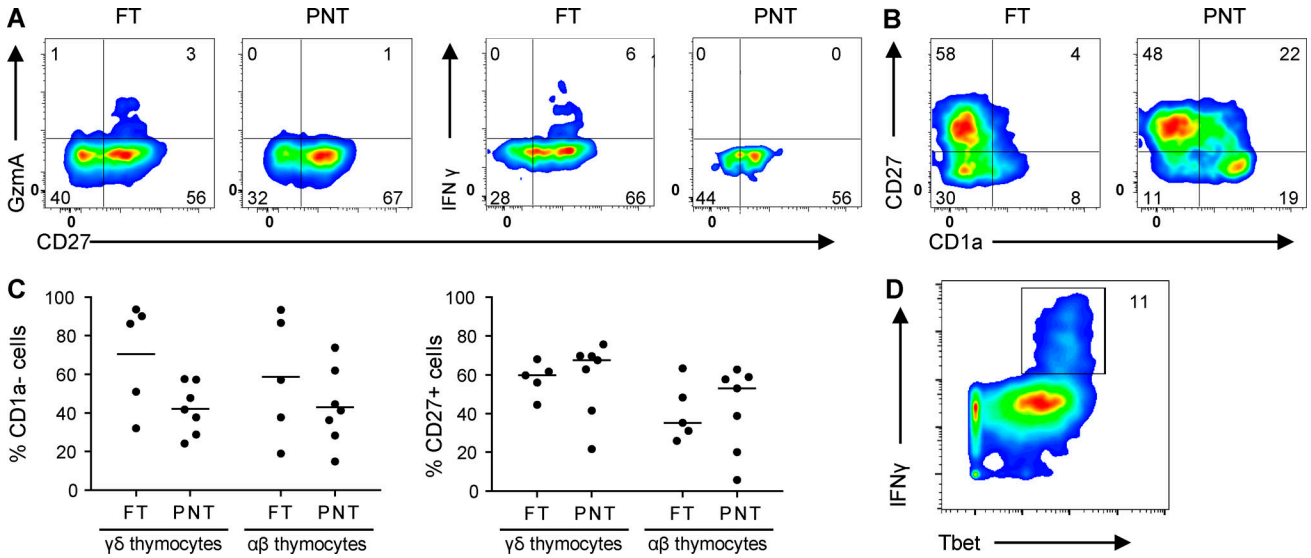

Figure S1. **Flow cytometry data on FT and PNT thymocytes. (A)** Flow cytometry plots of FT and PNT γδ thymocytes illustrating the expression of granzyme A$^+$ cells (left) and IFNγ$^+$ cells (right) within mature CD27$^+$ cells. **(B)** Flow cytometry plots illustrating the inverse relation of the expression of CD27 and CD1a maturation markers in FT and PNT γδ thymocytes. **(C)** Flow cytometry analysis of CD1a$^-$ (left) and CD27$^+$ (right) expression by fetal and postnatal γδ and αβ thymocytes. **(D)** Cytometry plot (based on CyToF data) of fetal γδ thymocytes illustrating IFNγ$^+$ cells within Tbet^{high} cells. Representative of five (FT) and six (PNT) independent experiments (A, left; and B) or representative of one (FT) and seven (PNT) independent experiments (A, right). Horizontal lines indicate medians. Flow cytometry plots (A and B) and data (C) represent FT and PNT γδ thymocytes without the Vγ9Vδ2 subset.

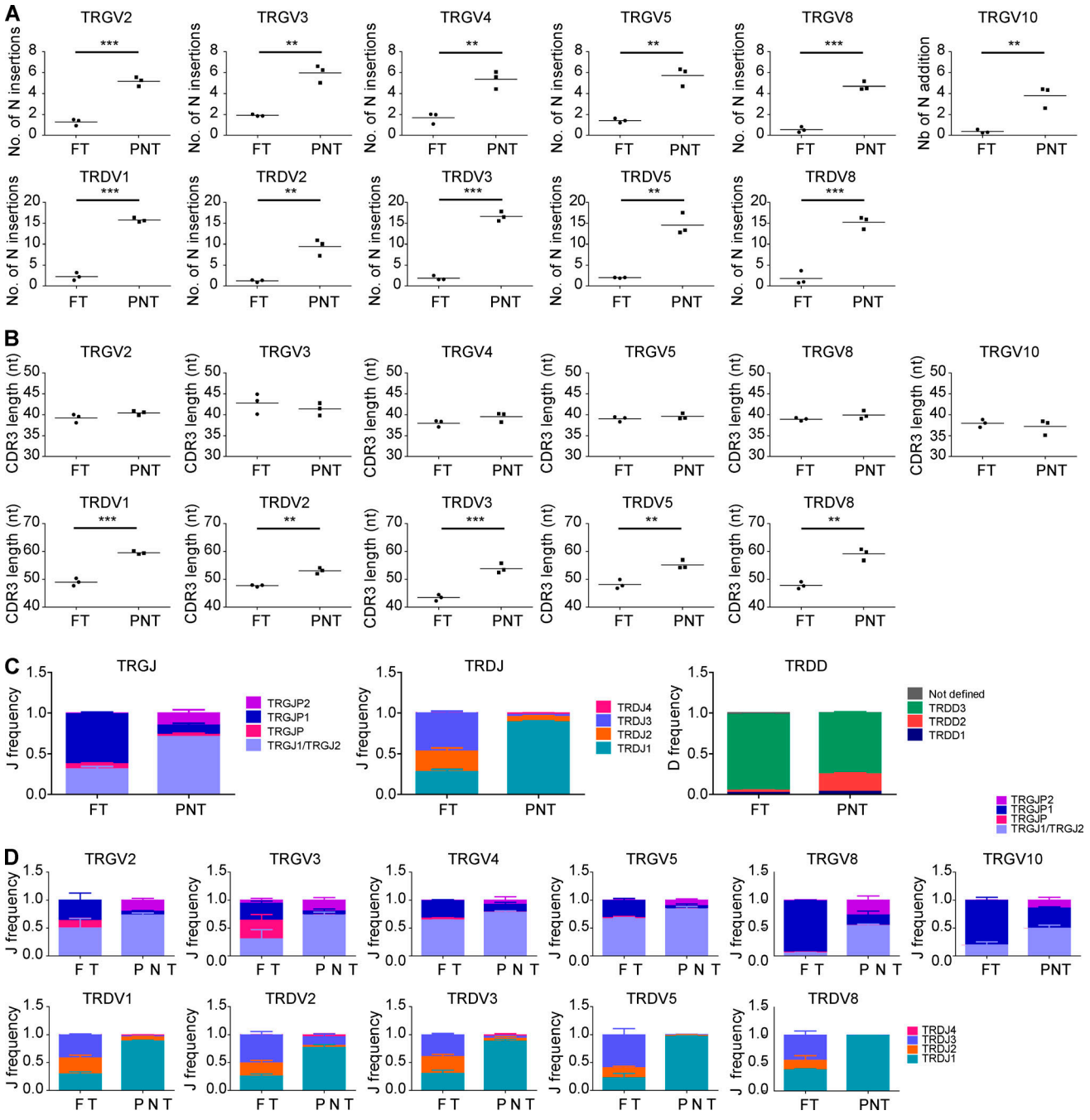

Figure S2. **TCR/CDR3 data of FT and PNT γδ thymocytes. (A and B)** Number of N insertions (A) and CDR3 length (B; number of nucleotides) of CDR3 containing the indicated TRGV and TRDV, from sorted FT and PNT γδ thymocytes. **(C)** J and D gene segment usage in TRG and TRD of sorted FT and PNT γδ thymocytes. **(D)** J gene segment usage in TRGV2, TRGV3, TRGV4, TRGV5, TRGV8, TRGV10, TRDV1, TRDV2, TRDV3, TRDV5, and TRDV8 of sorted FT and PNT γδ thymocytes. *n* = 3 for FT and PNT nonVγ9Vδ2 sorted γδ thymocytes. Horizontal lines in A and B indicate means; means ± SEM are shown in C and D. Data were analyzed by Student's *t* test; **, P < 0.01; ***, P < 0.001.

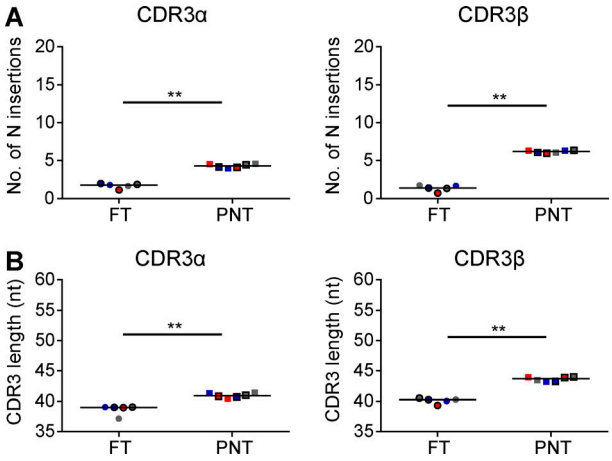

Figure S3. **CDR3 data on αβ thymocytes. (A and B)** Number of N insertions (A) and CDR3 length (B; number of nucleotides) in CDR3α and CDR3β repertoires of αβ thymocytes derived from FTs and PNTs. Colors represent replicates from the same subject with 10,000 αβ thymocytes (circles [FTs] and squares [PNTs] with black border) or 100,000 αβ thymocytes (circles [FTs] and squares [PNTs]). Horizontal lines indicate medians. Data were analyzed by Mann Whitney test; **, P < 0.01.

R1 read

AAGCAGTGGTATCAACGCAGAGTAC**ATG**GGGGTCACTGCT
GGAAGCATTTGCCTTCTCCTCCTGGGCTC*CTGACTTGCTGT*
*CCGAACATTTCAGTCTAGCTGCG**TGA**CCAAAATCATTCTTCA*
ATGTTTCCCTCTTCTACTGTCAGATGTT

ATG: first ATG in the TRGV10 RNA (start codon)
Italic and blue: presence of leader intron (Zhang 1994 EJI)
TGA: stop codon introduced in the TRGV10 because of absence of splicing of the leader intron

R2 read

AATAGTGGGCTTGGGGGAAACATCTGCATCAAGTTGTTTATC
AGGTGAAGTTACTATGAGCTTAGTCCCTTCAGCAAATATCTT
GAACCAACCAGTGGTATCCCACGCAGCACAGTAGTAAACG
GCCATGTCTTCTTTCTCTACGGACTTG

Orange: nucleotype corresponding the invariant germline-encoded TRVG10-TRGJP1 CAAWDTTGWFKIF CDR3 sequence

Figure S4. **TRDV10 RNA contains the leader intron introducing a stop codon.** Shown are the R1 and R2 raw data reads of a TRGV10-containing sequence that possesses the invariant germline-encoded CDR3 CAAWDTTGWFKIF.

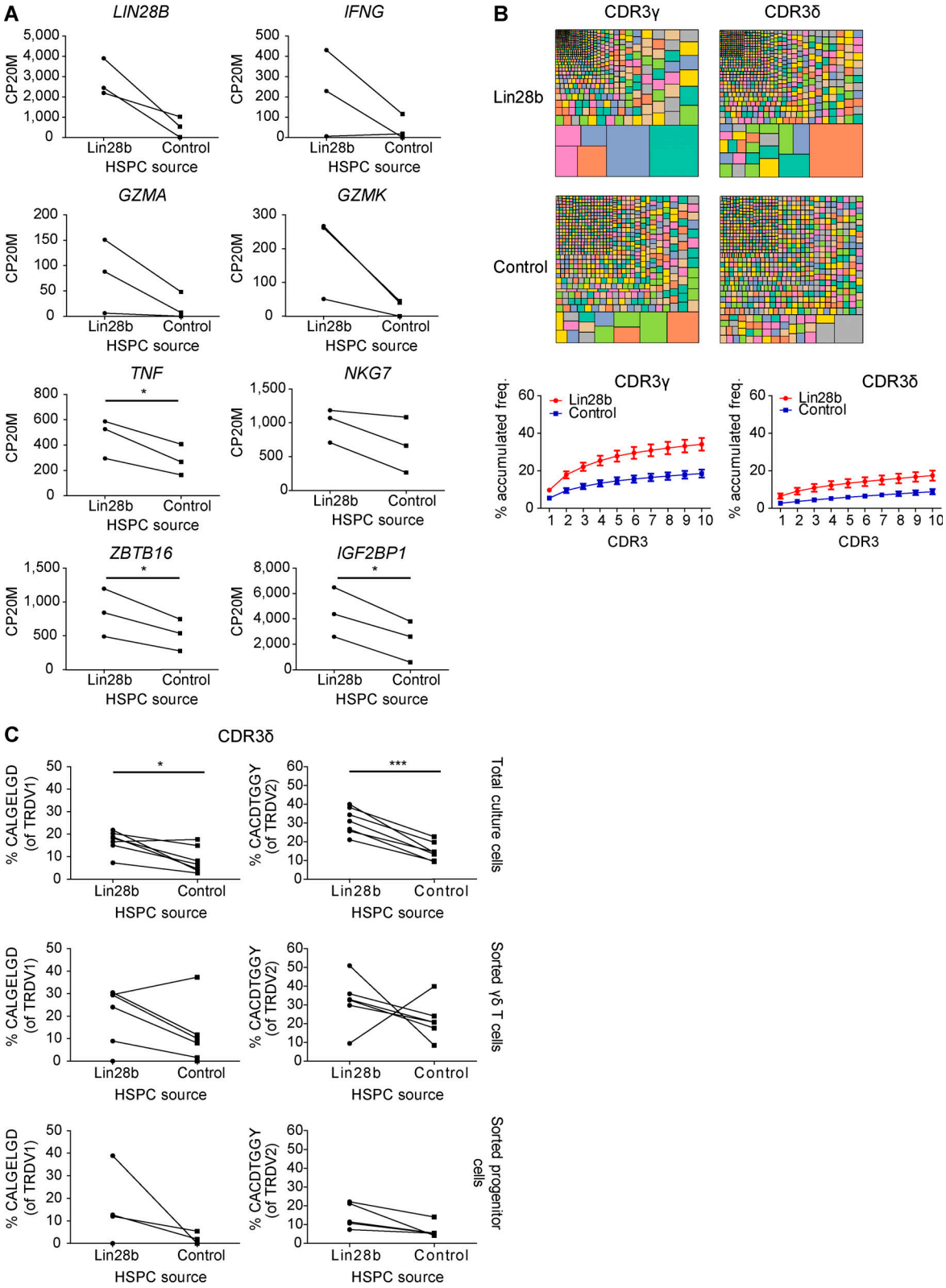

Figure S5. **TCR/CDR3 and RNAseq data of Lin28b- versus control-transduced CB HSPC-derived γδ T cells. (A)** Paired comparison analysis of the CP20M (RNAseq data) for a selection of genes expressed in γδ T cells derived from Lin28b- versus control-transduced CB HSPCs. **(B)** Tree map representations (colors used are random; no correspondence between graph; top) and accumulated frequencies (freq.; bottom) of the 10 most abundant clonotypes of the CDR3γ and CDR3δ repertoires of total cells derived from OP9DL1 culture. Tree maps are representative of seven (Lin28b and control) independent experiments. Graphs show the means ± SEM. **(C)** Percentage of particular CDR3δ clonotype amino acid sequences present in total cells, sorted γδ T cells, and sorted progenitor cells derived from Lin28b- versus control-transduced CB HSPCs. $n = 7$ (for total) and $n = 5$ (for sorted γδ T cells and progenitors). Lines between symbols link samples from the same subject. Data were analyzed by paired Student's t test; *, $P < 0.05$; ***, $P < 0.001$.

Table S1 is provided online as a separate Excel file and shows a list of differentially expressed genes between FT and PNT γδ thymocytes and between FL and AB γδ T cells.